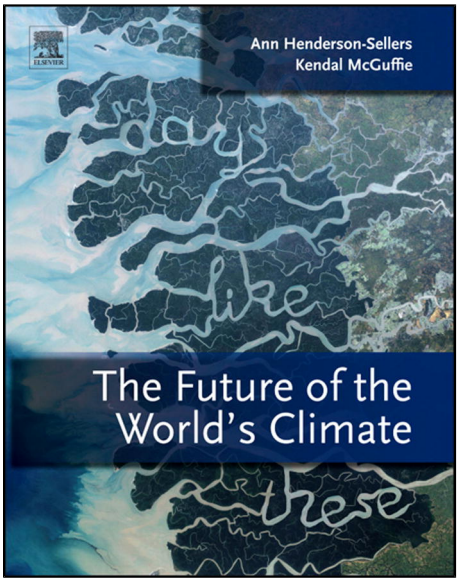

From Roger Barry, Regine Hock and Igor Polyakov (2012),The Future of the World's Glaciers, in The Future of the World's Climate, edited by A. Henderson-Sellers and K. McGuffie, pp. 197-222, Elsevier, Amsterdam.
ISBN: 9780123869173

Chapter 8

The Future of the World's Glaciers

Graham Cogley
Department of Geography, Trent University, Ontario, Canada

Chapter Outline

8.1. INTRODUCTION: CLIMATE AND THE CRYOSPHERE

8.1.1. Glaciers in the Context of Climatic Change

Glaciers are perennial masses of ice, and possibly firn and snow, originating on land by the recrystallization of snow and showing evidence of past or present flow (Cogley et al., 2011). They range in size from tiny but numerous glacierets, which differ from perennial snowpatches only in showing evidence of flow, to the Greenland Ice Sheet (area 1.7 Mm^2; 1 $Mm^2 = 10^6$ $km^2 = 10^{12}$ m^2) and the Antarctic Ice Sheet (area 12.3 Mm^2). Collectively, glaciers account for the bulk of the cryosphere, which also contains the world's ice shelves (another 1.5 Mm^2 of thick but floating ice), sea ice, lake and river ice, ground ice (in permafrost), and seasonal snowpacks. Glaciers have radiation balances, energy balances, and mass balances, like any study volume, and they exchange radiation, energy, and mass with other compartments of the near-surface environment, principally the atmosphere and the ocean, but also the aquifers in which much of the Earth's stock of water is stored. In addition, they interact with the Earth's mantle because of its viscoelastic response to loading at the surface, and with the rest of the Earth as a whole through the effect on the gravitational field of their exchanges of mass with the ocean (Peltier, 2004).

Changes in the extent and mass of glacier ice are, in a naive view, 'caused' by changes in the climate. In truth, the direction of causality is not necessarily well-defined. Frozen water is the brightest, and liquid water among the darkest, of the materials at the Earth's surface. Sufficiently large changes in the relative proportions of the two phases can feed back on the climate that appears to have caused the

The Future of the World's Climate. DOI: 10.1016/B978-0-12-386917-3.00008-7

changes. The phenomenon of ice–albedo feedback has been a fundamental feature of our understanding of the Earth's radiation and energy balances since it was first elucidated by Sellers (1969) and Budyko (1968).

A measurement of the mass balance of a glacier involves no assumptions about temperature. Glaciers are therefore environmental and climatic monitoring devices that are physically independent of the weather stations and of bathythermographs. The greater number of temperature measurements, the availability of abundant information about temperature in the form of atmospheric reanalyses and climate projections, and the observed correlation of mass balance with temperature, which is invariably found to be strong, combine to make temperature-index modelling (Hock, 2003) a natural way to explore present and future glacier changes. However, glaciers would yield reliable information about environmental change, and in particular about changes in the radiation balance, even if the thermometer had never been invented.

The information is of course different in kind from that in temperature records. The glacier's annual mass balance, apart from possible losses by iceberg calving, is a response to climatic forcing integrated over the year, over the area covered by the glacier and over its vertical extent. Thus, the glacier is an insensitive, but not therefore a less valuable, indicator of climatic change. Glaciers also sample different parts of the Earth's surface, being found at higher altitudes and latitudes than most weather stations.

8.1.2. Glaciers in the Context of Socio-Economic Change

The mass of fresh water stored in glaciers was about 25.5 million Gt in the late twentieth century, with all but about 0.2 million Gt in the two ice sheets. Of the ice in glaciers other than the ice sheets, most is in uninhabited or thinly peopled drainage basins at high polar latitudes. Nevertheless, there are many catchments in which glacier ice is a significant human resource. For example, glaciers fuel hydroelectric power stations in Norway and other countries; yield fresh water for irrigation and domestic consumption in Canada, Peru, Pakistan, and China; attract tourists to Switzerland, Kenya, Nepal, and the Antarctic; and are icons of the wilderness for billions of city dwellers – you have to traverse one glacier or another if you aspire to climb Mt Everest or K2 and, although they are likely to disappear in the next few decades, glaciers persist today at the summit of Kilimanjaro.

In populated drainage basins, the glaciers may pose a significant hazard to those living downstream. *Jökulhlaup* is an Icelandic word that translates as 'glacier burst' and refers to sudden, very large increases in the discharge of glacier meltwater streams. Some glaciers dam meltwater lakes in marginal valleys. If the meltwater becomes so deep that the ice dam floats, there is an abrupt, potentially catastrophic increase in discharge, followed by a recession and ultimately a return to low rates of flow. Subglacial volcanic eruptions are especially hazardous because of the large volumes of meltwater that result, and sometimes because of lahars, rapid and damaging mudflows. The lahars of the 1985 eruption of Nevado del Ruiz in Colombia were responsible for most of the 23,000 resulting deaths. Lliboutry et al. (1977) and Arnao (1998) document the known history of glaciogenic lahars and avalanches in Peru that, in sum, have killed tens of thousands of people. Many of these catastrophes are due to the failure of moraines damming proglacial lakes, a hazard that impends also over many glacierized valleys in the Himalaya (Fujita et al., 2009). The hazard can be understood in terms of glacier retreat from advanced positions attained during the Little Ice Age and marked today by the terminal moraines. Avalanches from valley walls and calving events at the glacier terminus generate lake-water surges that trigger failure. Richardson and Reynolds (2000) noted that the frequency of moraine-dam failures in central Asia appears to be increasing. It is unlikely that the increase in frequency could be shown to be statistically significant, but the hazard remains serious and the explanation for it remains obvious.

The most significant way in which glaciers impact society indirectly is through their contributions to the water balance of the ocean or in other words, in the modern context, to sea-level rise. A sea-level rise of as little as a metre may prove fatal to the aspirations of countries whose highest point is only a few metres above the mean sea level of the date at which they became independent. The same sea-level rise would be colossally expensive for older and for more highly-developed countries. And if a substantial portion of the nearly 26 million Gt of water now in glaciers were transferred to the ocean, we would have to choose between the end of civilization as we know it and the physical relocation of civilization to a position at least 80 metres higher than at the present day.

8.1.3. Scope

In what follows, we will first set out the elements of an understanding of what glaciers are and of how they exchange energy with their surroundings (Section 8.2). The focus will then narrow in Section 8.3 to exchanges of mass, because there is far more information on mass balances than on energy balances and because our physical understanding assures us that there is an equivalency, to a good approximation, between mass exchange and energy exchange. Section 8.4 is about the tools with which glaciologists model those attributes of glaciers that are difficult or impossible to measure, or that require to be projected as responses to anticipated environmental change. The initial conditions for these models, including present-day states

and rates of change, are of basic importance, and they are the subject of Section 8.5. Section 8.6 is an assessment of recent assessments of future mass losses from glaciers, while Section 8.7 offers concluding reflections.

To keep this survey within manageable limits, the two ice sheets are considered only briefly, and mainly for comparative purposes. For brevity and clarity, the glaciers other than the ice sheets are sometimes referred to as 'small glaciers', but with no implication that they are small by any measure other than that provided by the ice sheets.

8.2. ELEMENTS

8.2.1. Glacier Geography and Physiography

Glaciers are bounded by continuous outlines, parts of which, called divides because the ice flow diverges there, may be shared with adjacent glaciers. Thus, an ice cap, which may be a unit for climatological purposes, is sometimes subdivided for glaciological purposes into several glaciers. The glacier margin is that part of the outline that is in contact not with an adjacent glacier, but with unglacierized terrain or possibly with sea or lake water. Where the ice flow produces an elongate tongue, as in valley glaciers and often in outlet glaciers of ice caps and larger bodies, the margin is called the terminus. Some glaciers have floating tongues, and some nourish ice shelves; here, the grounding line, where the condition for flotation is satisfied, is a significant part of the margin. The condition for flotation of ice of thickness h in water of depth d is $d = h\,\rho_i/\rho_w$, where ρ_i is the density of the ice and ρ_w the density of the water.

In any vertical column through a glacier, the uppermost parts are likely to consist not of glacier ice but of firn and snow. Snow is solid precipitation that has accumulated during the current balance year. By convention, snow becomes firn instantaneously at the end of the balance year. Firn, then, is snow that has survived at least one season of ablation (mass loss), but has not been compacted to a density near that of pure ice.

Typical glaciers have vertical extents of hundreds and sometimes thousands of metres. Differences of mean temperature of several kelvins between the lowest and highest points on the glacier surface are therefore usual. The components of the local or point mass balance (the change of mass of a vertical column extending through the glacier, over a given span of time) vary greatly between the minimum and maximum elevations (Figure 8.1), so it is instructive and useful to subdivide the glacier into zones (Figure 8.2). Most glaciers have an accumulation zone at higher elevation, where annual mass gain, mainly by snowfall, exceeds annual mass loss, mainly by melting, and an ablation zone at lower elevation, where annual mass loss, possibly including losses by calving, exceeds annual mass gain. Processes of accumulation (mass gain) and ablation (mass loss), other than those just mentioned, include sublimation and deposition of vapour, redistribution by the wind, and avalanching, but these are seldom dominant and often unimportant.

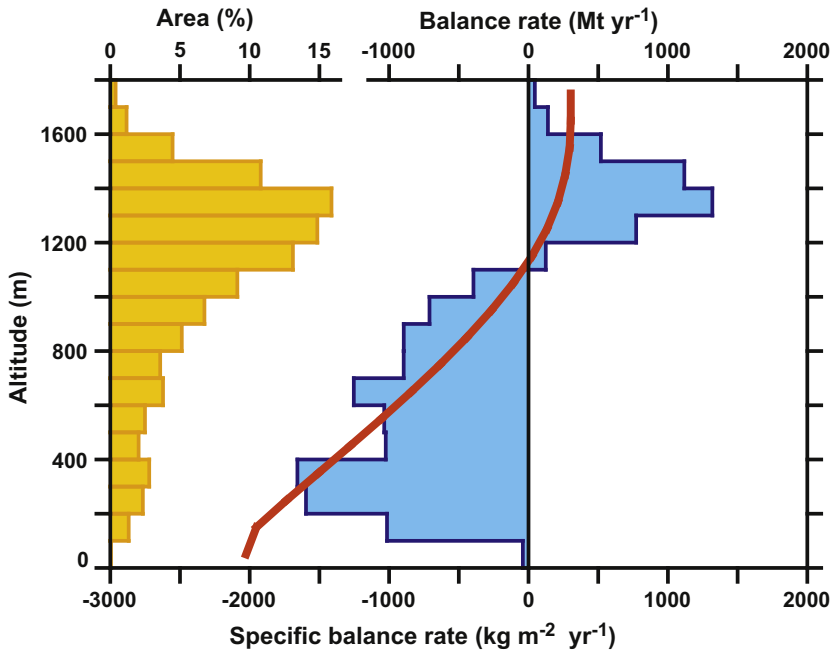

FIGURE 8.1 Hypsometry (distribution of area with altitude; yellow histogram), specific balance rate (red line), and balance rate (blue histogram) of White Glacier in arctic Canada (area 39.4 km^2). The specific balance, $b(z)$, is the local sum of accumulation, $c(z)$, and ablation, $a(z)$. Balance data are averages for 1959/60 to 2008/09. The glacier-wide specific balance (the area-weighted average of the red line) was -175 kg m^{-2} yr^{-1} on average over the measurement period. The blue histogram is the product of the yellow histogram and the red line and shows that balance magnitudes are largest where relative area is least.

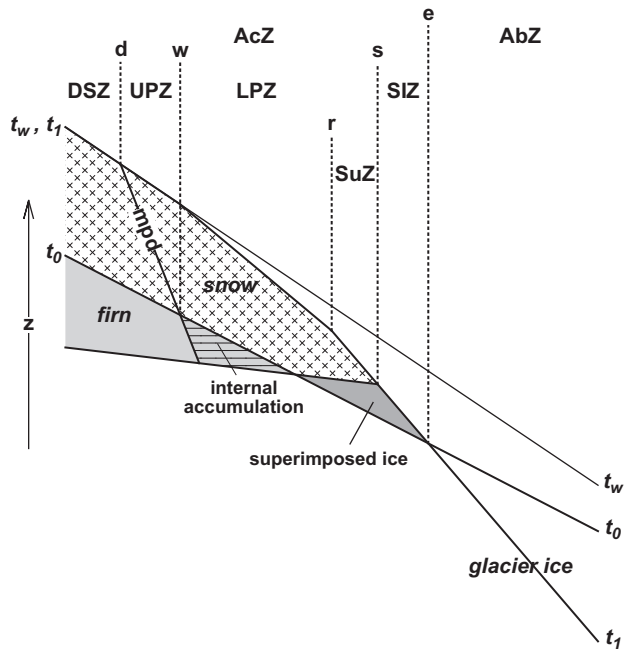

FIGURE 8.2 Glacier zonation and its balance-related aspects on a representative cold or polythermal glacier. At the start of each mass-balance year, the glacier surface is at the line $t_0 - t_0$. It evolves (schematically, the effects of ice flow being neglected) to $t_w - t_w$ at the end of the accumulation season, when the mass of the glacier reaches its annual maximum, and then to $t_1 - t_1$ at the end of the ablation season, when it becomes the summer surface of the next balance year. 'mpd' is the maximum depth to which meltwater percolates before refreezing. The zones are AbZ: ablation zone (the zone below e); AcZ: accumulation zone (all the zones above e); SIZ: superimposed ice zone; SuZ: slush zone, a part of LPZ; UPZ: upper percolation zone; LPZ: lower percolation zone or wet-snow zone; DSZ: dry-snow zone. The zones are separated by the lines e: equilibrium line; s: snowline; r: runoff limit or slush limit (position variable, depending especially on the surface slope); w: wet-snow line (intercept of mpd on summer surface, separating UPZ and LPZ); d: dry-snow line (surface outcrop of mpd). *(Source: "Glossary of Glacier Mass Balance and related Terms", IHP-VII Technical Documents in Hydrology, No2, Figure no 16, p.101, Cogley et al., © UNESCO/IHP 2011. Used by permission of UNESCO.)*

On some glaciers, particularly those in cold climates, it makes sense to subdivide the accumulation zone further, as in Figure 8.2. The dry-snow zone, for example, is the part of the glacier where there is no surface melting. Most glaciers have no dry-snow zone, but the dry-snow zone extends over almost all of the Antarctic Ice Sheet and (until recently) about half of the Greenland Ice Sheet. The superimposed ice zone is the part of the glacier where, at the end of summer, the surface consists of superimposed ice, which is meltwater that has percolated to the base of the winter snowpack and refrozen. The superimposed ice zone, if present, separates the ablation zone from the percolation zone, its upper boundary being the snowline and its lower boundary the equilibrium line. This distinction can be important, for example in attempts to assess mass balance remotely. Superimposed ice is mass gained during the current mass-balance year, but is extremely difficult to tell apart from the old glacier ice that is exposed below the equilibrium line.

The mass-balance year is only roughly as long as a calendar year. It extends from one annual minimum of mass at the start of winter (September or October, March or April, depending on latitude and hemisphere) to the next annual minimum at the end of the following summer.

Glaciers are distributed widely across the Earth's surface, with an overwhelming concentration near the poles (Figure 8.3). The annual equilibrium line, as observed at the end of each balance year, separates the accumulation zone from the ablation zone. Its mean altitude, abbreviated ELA, is both a fundamental physiographic attribute of the glacier and a valuable descriptor of glacier climate and geography. As shown in Figure 8.4, the ELA reaches sea level at and poleward of about 60°–65°S, and approaches, but does not reach, sea level at the North Pole. It rises above 6 km in the desert belts and is depressed in the region through which the Inter-Tropical Convergence Zone migrates seasonally, to below 5 km in places. At equivalent extra-tropical latitudes, the ELA is up to several hundred metres lower in the Southern Hemisphere than the Northern. In the mid-latitudes, there are moderate but visible depressions of the ELA that can be understood as responses to enhanced accumulation beneath the polar front of each hemisphere. The distribution of warmest-month temperature at the ELA reinforces this interpretation. The greater the annual accumulation, the greater the annual ablation must be in order to remove the annual accumulation exactly. Greater ablation requires warmer temperatures and, therefore, a lower ELA. (By definition, surface accumulation and ablation are equal at the ELA.) In a warming climate, the ELA is expected to rise. However, the annual accumulation is also expected to increase in places where it is already substantial, and the annual ablation by melting and sublimation is expected to become more negative where evaporation is already substantial. This expectation translates into a more curvaceous version of Figure 8.4, but it has not yet been detected (or searched for).

As the ELA rises during a period of greater radiative energy gain, or falls during a period of increased accumulation, so the glacier responds, not only by losing or gaining mass, but also by adjusting its size dynamically. Glacier dynamics is not the central concern of the present study, but it is a profoundly important subplot in the narrative of glacier change (cf. Lenton, 2012, this volume). The glacier always seeks equilibrium with its climatic forcing, but always requires years to millennia, depending on its size, to attain that equilibrium (Jóhannesson et al., 1989). So the climatic information in records of glacier change is integrated not just over the glacier's horizontal and vertical extent, and not just over seasonal time, but also over secular time.

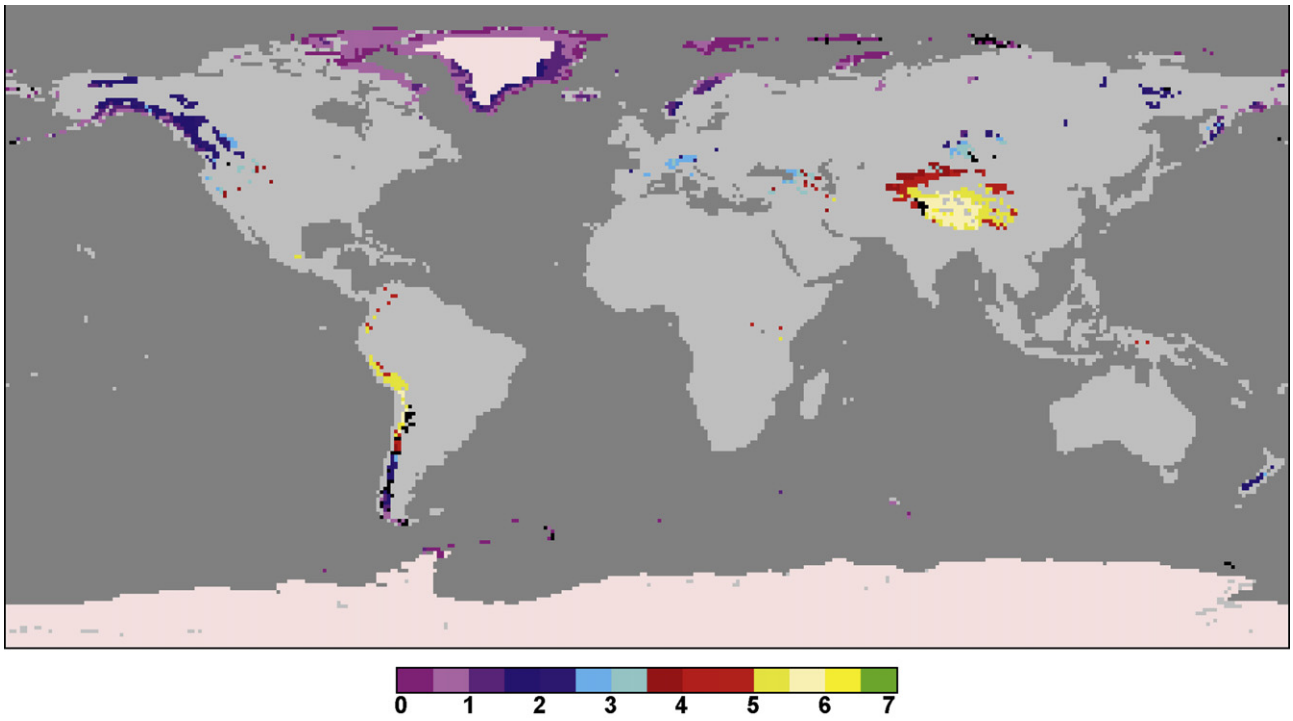

FIGURE 8.3 Geographical variation of the equilibrium-line altitude (ELA) in km, as approximated by averages within 1° × 1° cells of glacier midrange altitudes from the World Glacier Inventory and other sources. The midrange altitude is the average of the glacier's minimum and maximum altitudes, and approximates the ELA well at this scale (Cogley and McIntyre, 2003). Ice sheets, for which the ELA is not estimated, are light pink; ice-free land is light grey; and glacierized cells lacking information on their ELA are black.

The accumulation-area ratio, abbreviated AAR and symbolized as α, is closely related to the ELA and to the mass balance. It is equal to the area, S_c, of the accumulation zone divided by the area, S, of the glacier, $\alpha = S_c / S$. The AAR is bounded between 0 and 1. An α of 1 requires that the glacier lose mass entirely by frontal ablation, as is nearly true of the Antarctic Ice Sheet. An α of 0 implies that the ELA is above the maximum

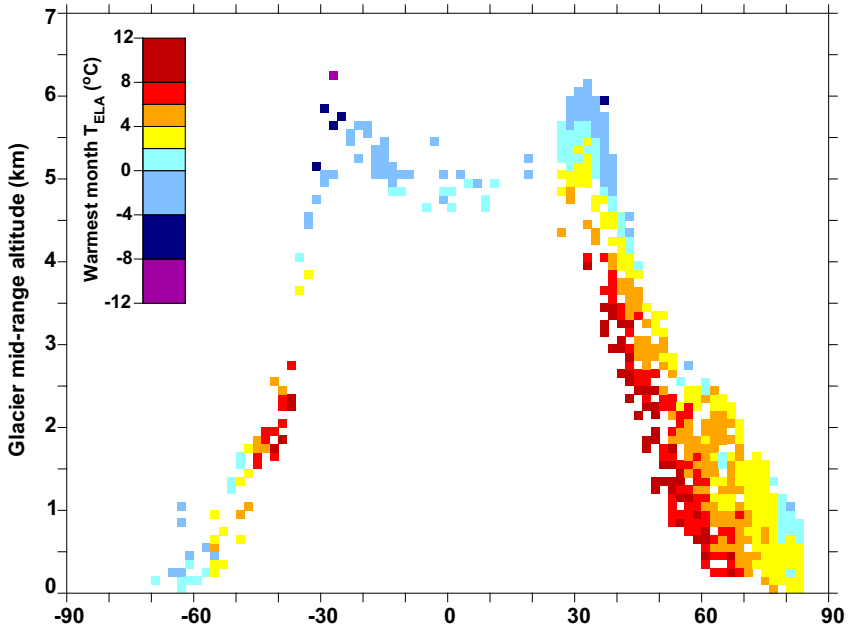

FIGURE 8.4 The ELA as a function of latitude. The information of Figure 8.3 is assembled into cells spanning 2° in latitude and 100 m in altitude, then coloured by averaging climatological averages from a reanalysis for 1968–1996 (Kalnay et al., 1996) of the free-air temperature of the warmest month at ELAs falling within each cell.

elevation of the glacier, which will dwindle and eventually vanish if the state $\alpha = 0$ persists. On glaciers with no frontal ablation, annual AAR is always well-correlated linearly with annual mass balance. Smaller AAR implies more negative mass balance. The AAR plays an essential part in one of the projections of glacier evolution during the twenty-first century, to be discussed in Section 8.6.1.

Glacier ice that is at its pressure-melting point is said to be temperate, while glacier ice below the pressure-melting point is said to be cold. Neglecting seasonal warming and cooling near the surface, a column of ice that is partly temperate and partly cold is said to be polythermal. The three adjectives are often applied to entire glaciers. The adjectival distinction is significant. For example, temperate ice is likely to transmit surface meltwater. However, should it percolate to a cold part of the column, the meltwater will refreeze. Furthermore, basal sliding is likely to contribute significantly to the rate of ice flow if the glacier is wet-based (its bed is temperate) but not if it is dry-based (its bed is cold).

8.2.2. The Radiation Balance

Glaciers have radiation balances exactly like those of other natural and constructed surfaces:

$$R_n = (1 - \alpha_s)K_\downarrow + I_a - \varepsilon\,\sigma T_s^4 \qquad (8.1)$$

where the net radiation, R_n, is the sum of the absorbed solar irradiance (the incident irradiance, $K_\downarrow$, multiplied by 1 minus the surface albedo α_s) and the incident downwelling radiation from the atmosphere, I_a, minus the surface emittance. The surface emittance is proportional to the fourth power of surface temperature T_s. The Stefan–Boltzmann constant, σ, is equal to 5.67×10^{-8} W m^{-2} K^{-4}. Snow and ice are usually treated as black bodies, that is, their emissivity, ε, is assumed to be 1.

Glaciers are distinctive among natural surfaces in that their surface albedo is typically high, although debris cover can eliminate this difference. Exposed glacier ice is usually darker than snow. Snow, if fresh, may absorb three times less solar radiation than the ice that it covers, and its seasonal disappearance is followed by a marked shift in the energy balance to a more absorbent regime in which, other things being equal, melting is accelerated. For present purposes, however, the main radiative peculiarity of glaciers is that their temperature is no greater than the pressure-melting temperature, T_m, which is equal to 273.15 K at the surface, so that the surface emittance is no greater than about 316 W m^{-2}. It can be much lower in winter and at night, and net gain of infrared radiative energy is not unusual on glaciers.

8.2.3. The Energy Balance

The energy balance at the surface of a glacier is:

$$R_n + H + L_v E + G_s + L_f A_s = 0 \qquad (8.2)$$

where all the quantities are flux densities (that is, in W m^{-2}), positive when directed towards the surface. R_n is the net radiation from Equation (8.1). H and $L_v E$ are turbulent fluxes of sensible and latent heat respectively from the air; $L_v = 2.834$ MJ kg^{-1} is the latent heat of sublimation. G_s is the conductive flux of heat from beneath the surface. Finally, $L_f A_s$ represents the energy used for surface melting, with $L_f = 0.334$ MJ kg^{-1} the latent heat of fusion and A_s the surface meltwater flux (kg m^{-2} s^{-1}).

Because the air above glaciers is often warmer than the freezing point in summer, and is often a heat source fuelling radiative cooling of the surface in winter and at night, the sensible heat flux is generally directed downwards. The latent heat flux is often directed downwards also because the vapour pressure at the surface will be that appropriate to saturation at a temperature below T_m, or at T_m if meltwater is present. On the lower parts of glaciers, the turbulent fluxes are enhanced by katabatic drainage of cooled air from high elevations. The katabatic wind, as well as being persistent and directionally constant, can be extremely strong and an important component of the local climate (cf. Evans et al., 2012, this volume).

The heat exchanged with the interior of the glacier drives an annual variation of temperature that is confined to the upper 10 m–15 m. However, in summertime, if and when an isothermal surface layer at the freezing point has been established, the heat flux, G_s, must dwindle to zero and any surplus from the atmospheric terms in Equation (8.2) will be used for melting. This surplus is responsible for most of the ablation on most glaciers, exceeding −10,000 kg m^{-2} yr^{-1} (about −100 W m^{-2}) near glacier terminuses in lower latitudes. It may be responsible for advective heat transfer, $\rho_w L_f u_p$, where u_p is the vertical percolation rate, to the interior of the glacier if the meltwater refreezes at depth instead of running off.

Glaciers also have basal energy balances. The energy sources at grounded glacier beds are frictional heat and geothermal heat. Geothermal heat fluxes are of the order of 0.05 to 0.10 W m^{-2}. Frictional heating derives from the loss of potential energy in the ice column as it moves downslope. Its rate can be expressed as the product of basal velocity and basal shear stress, yielding typical fluxes of 0.01 to 1 W m^{-2}. These fluxes are small, 0.1 W m^{-2} being equivalent to −10 kg m^{-2} yr^{-1} of basal melting, but they represent heat sources without compensating sinks, so they tend to make cold glaciers steadily warmer. Once the basal ice has reached its pressure-melting temperature, upward conduction into the

body of the glacier ceases and the available energy is used to melt ice. This accounts for one of glaciology's bigger surprises: that the beds of many glaciers, including large parts of the beds of the ice sheets in Greenland and Antarctica, are wet. The pressure-melting point of water saturated with air decreases at -0.86 K km^{-1}, such that, beneath 4000 m of ice, T_m is 3.4 K below its value at the surface (Cogley et al., 2011).

The basal energy balance can be profoundly different when the ice is afloat (Holland and Jenkins, 1999). The frontal energy balance may become significant when a grounded terminus is in contact with sea water or lake water. Most of the concern centres on tidewater glaciers, that is, those in contact with seawater. The principal controls on the basal energy balance are the properties 'imported' by the meso-scale water flow. Warm water, more or less salty, can be advected to the neighbourhood of the glacier by currents. The resulting convective heat transfer to the ice can be substantial. The ice-water contact is at the temperature T_m, which depends on the pressure of the overlying ice (or the water depth at a grounded terminus) and the salinity of the water. There are two complications. Firstly, salt is coupled to heat because freezing increases and melting decreases the salinity of the seawater, altering both T_m and the buoyancy of the water. Secondly, the water flow itself is driven substantially by variations of temperature and salinity. The meltwater is buoyant because it is fresh, and flows upwards along the base of the rapidly-thinning ice to where a lesser pressure implies higher T_m and lesser sensible heat transfer. Sometimes, the meltwater flows into an environment that is actually colder than T_m, and ice begins to form, accreting as 'marine ice'.

Direct measurements are very difficult, but Rignot and Jacobs (2002) have measured West Antarctic basal melting rates indirectly at 23 grounding lines. These rates pertain only to areas of limited extent, but they are extremely high. The greatest recorded magnitude, 425 W m^{-2} at Pine Island Glacier, entails the melting of 44 m of ice per year because conduction of heat upwards into the glacier is unlikely to be significant (Cogley, 2005). More recently, Rignot et al. (2010) have reported rates of frontal melting at outlet glaciers in Greenland that are highly variable, but are comparable with rates of calving. The significance of this rapid basal and frontal melting for the force balance of the ice extends far upglacier, because it 'pulls' grounded ice across the grounding line.

A concern with energy fluxes at the bottom of the glacier, hundreds or thousands of metres below the surface, may seem out of place in a book about the climate. But, whether the basal ice is grounded or afloat, lack of understanding of these basal energy exchanges is the fundamental reason for our inability to describe, let alone to predict, how the ice sheets and other tidewater glaciers respond to climatic forcing.

8.3. GLACIER MASS BALANCE

8.3.1. Terms in the Mass-Balance Equation

The mass balance, ΔM, is the change in the mass of the glacier, or part of the glacier, over a stated span of time. It is the sum of accumulation, C (all gains of mass), and ablation, A (all losses of mass, treated as negative quantities):

$$\Delta M = C + A \tag{8.3}$$

However, the relevant processes can be distinguished more clearly if it is written as:

$$\Delta M = B + A_f \tag{8.4}$$

where, in the terminology of Cogley et al. (2011), B is the climatic-basal mass balance and A_f is frontal ablation. The climatic-basal balance is the sum over the extent of the glacier of the surface mass balance, the internal mass balance, and the basal mass balance. Frontal ablation is the sum of losses at the glacier margin by calving, subaerial melting, and sublimation and subaqueous melting.

The surface balance is more often measured than the other balance components, some of which it is not practical to measure while some are zero on many glaciers. The so-called glaciological method of in situ measurement of the surface mass balance relies on stakes and snow pits, and yields no information about the internal and basal balances. In geodetic measurements, the balance is estimated by repeated mapping. The change of glacier volume is obtained as the difference of glacier surface elevation, which is multiplied by an assumed average density to obtain the change of mass. Again, the measurement is ambiguous as to the internal and basal balances, and in particular as to internal accumulation, which can produce a decrease of volume due solely to the increase of density following from refreezing. Gravimetric observations with the GRACE satellites (e.g., Arendt et al., 2008) measure mass change directly, but have spatial resolution of the order of 200 to 300 km and do not resolve the components of the climatic-basal balance, or indeed of the total balance.

Accumulation by snowfall may be augmented by avalanching and vapour deposition, and may be diminished by wind scouring if the scouring is followed by either sublimation or transfer of the remobilized snow across the glacier outline (e.g., Bintanja, 1998). Avalanching can become a dominant term in the balance of very small glaciers in sheltered hollows. Such glaciers may, thus, be less reliable guides to the climate than more exposed glaciers, or at least different guides. An important anticipated consequence of the anthropogenically enhanced greenhouse effect is a more intense hydrological cycle, in which evaporation and precipitation both increase, but in geographically disparate ways. There is some evidence for this in observations (X.B. Zhang et al., 2007; Wentz et al.,

2007). Wentz et al. (2007), for example, show that both precipitable water and precipitation have increased recently, consistent with an expectation that, although the temperature has risen, the relative humidity should not change much. They point out, however, that, for reasons that remain unclear, the climate models tend to simulate more moderate increases in precipitation. Increased snowfall on glaciers is, nevertheless, an expected consequence of climatic change and has been detected on the ice sheets (e.g., Helsen et al., 2008). Trends in accumulation on smaller glaciers have not yet been studied.

Surface ablation occurs mainly by melting, although it should be noted that standard measurement methods would not distinguish between melting and sublimation if the latter were significant. The leading fact about surface ablation is that it is found to be proportional to elevation. Barring possible net losses due to sublimation or removal by the wind, ablation is zero at the dry snow line and decreases downwards along the surface to a minimum at the terminus. (Recall that ablation is negative.) The variation with elevation is often linear, as is that of surface temperature, helping to explain the success of temperature-index models at simulating ablation.

Internal accumulation is dominated by the refreezing of percolating meltwater in firn. It is negligible in temperate glaciers but is a difficult bias to control for in cold and polythermal glaciers, on which it is not detected by glaciological measurements. The main energy source for internal ablation is the potential energy released by downward motion of the flowing ice and of surface meltwater. This energy, and possibly some kinetic energy, is used to melt the walls of englacial conduits, and can sometimes contribute moderately to the climatic-basal mass balance of temperate glaciers. The magnitude of internal ablation has to be calculated rather than measured (Trabant and March, 1999), although it is often neglected.

There is no published estimate of the relative global extents of cold, polythermal, and temperate ice, but the temperature at 10 m to 15 m below the surface can be approximated by the mean annual surface air temperature, T_s, if there is no refreezing. Some internal accumulation should be expected wherever T_s is below the freezing point, which suggests that it is likely to be non-negligible in the upper parts of many glaciers that would be labelled as temperate. Its importance is generally acknowledged in modelling of the mass balance, but the parameterizations of refreezing are typically very simple and the values chosen for the parameters have very limited observational support. The most commonly made assumption is that the firn and the surviving snow have a capacity for refrozen meltwater that is proportional to the temperature. All surface meltwater goes to satisfy that capacity and, when it is reached, all subsequently produced meltwater runs off. An ambiguity between observations and models should be noted with respect to the terms 'internal accumulation' and 'refreezing'. The latter includes refreezing in the snow, which is generally detected in glaciological observations, while the former does not; the models generally do not distinguish between the two.

The basal mass balance is not measured but, at least for grounded ice, it can be calculated with a fair level of confidence. It is usually estimated to be a small contributor to the climatic-basal balance of grounded ice, although basal ablation and accumulation are major terms for floating ice.

Measurements of frontal ablation are difficult and are not made routinely. Calving, the mechanical detachment of blocks of ice, is an irregular and, at present, an unpredictable process. Except for dry calving from cliff-like terminuses on land, it is zero for land-terminating glaciers. It may be a significant balance component for lake-terminating glaciers but, on the global scale, calving is essentially a feature of tidewater glaciers and ice shelves. Where it has been evaluated reliably, for example by monitoring ice discharge through gates just upglacier from the calving margin, as well as advance or retreat of the margin, it has been found to be equal to a substantial fraction of the magnitude of total ablation.

There are two ambiguities to be aware of in respect of calving. Firstly, it is not necessarily the same as discharge across the grounding line, which may well be of more interest, especially if the concern is with changes of sea level. Discharge at the grounding line is more easily measured, for example by radar interferometry together with thickness measurements by radio echo sounding (Rignot et al., 2008). Secondly, it is sometimes said that estimates of average glacier mass balance are based only on measurements of the climatic-basal balance (often, just the surface balance) and neglect calving. Here, the verb 'neglect' is inaccurate and should be replaced by 'underrepresent'. For example, the three independent assessments that were combined by Kaser et al. (2006) are not based on any measurements that neglect calving. In terms of Equation (8.4), all of the measurements employed are of ΔM, not of B, and the problem is that there are many fewer measurements on glaciers with non-zero A_f. Cogley (2009a) produced circumstantial evidence that calving glaciers have more negative mass balance than others at the present day, but it remains challenging to produce routine large-scale estimates that are not biased by the shortage of measurements of frontal ablation.

Subaerial frontal melting and sublimation have been little studied. They are likely to be insignificant by comparison with the subaqueous frontal melting documented by Rignot et al. (2010). Heat transfer from water to ice can be far more efficient than transfer from the air. Evidence for the incursion of warmer seawater into sub-ice cavities in West Antarctica was first produced by Rignot

and Jacobs (2002), but more dramatic incursions into Greenland fiords have been documented (and dated) recently by Holland et al. (2008) – see also Straneo et al. (2010). These publications have exposed a major gap in understanding of the role of the ocean as a trigger, via frontal ablation, for rapid change in the mass balance and dynamics of tidewater glaciers. Most land-terminating glaciers do not have the cliff-like terminus that is a prerequisite for separating the frontal balance from the surface balance. Of those that do, the plateau glaciers on Kilimanjaro are notable for the protracted retreat of their vertical walls (Cullen et al., 2006).

8.3.2. Definitions and Units

The time span of a mass balance is never separable from the mass change and must always be stated, but whether to express the mass change as a magnitude or a rate (by dividing the change by the time span) is a matter of expediency. In this study, most balances are expressed as rates. The year is a natural choice for the unit of time, although the day is sometimes more convenient.

Cogley et al. (2011) explain the units that are used in glaciology. In particular, 'specific' means 'per unit area'. A specific mass balance is a mass balance per unit of horizontally-projected area. Specific units (such as kg m^{-2}) are valuable in comparing point mass balances in different parts of the glacier, in comparing glaciers one with another, and in assessing the relations between mass-balance components and the mass and energy flux densities that constitute the forcing for the mass balance. The often-seen mm w.e. (millimetre of water equivalent) is numerically identical to the kilogram per square metre.

In climatology, and in studies of the ice sheets, dates usually contain calendar years. As a reminder that mass-balance calculations for glaciers other than the ice sheets nearly always refer to mass-balance years, beginning in September or October in the Northern Hemisphere, dates that refer to mass-balance years are given here in the form *yyss/tt*, where *tt* is greater by 1 than *ss* and denotes the calendar year in which the mass-balance year ends.

For the analysis of mass exchange between the glaciers and other stores of water in the hydrosphere, such as the ocean, specific quantities must be converted to totals in units such as kg or Gt. As a convenience, however, many of the mass balances and masses herein are expressed as sea-level equivalents, m SLE or mm SLE. A mass of water or ice can be converted to m SLE, itself a specific unit, by dividing by the product of the density of fresh water, 1000 kg m^{-3}, and the area of the ocean, 362.5 Mm^2 (Cogley et al., 2011), with a change of sign, when necessary. More explicitly, 1 Gt = 10^{12} kg = 1.0/362.5 mm SLE. This conversion fails to allow for the viscoelastic response of the solid earth to differential loading, but that response has a timescale of several thousand years and is of no consequence for present purposes. The conversion also assumes that the ice is not grounded below sea level and therefore already partly displacing ocean water; that the area of the ocean is not altered by shoreline or grounding-line migration; and that mass lost by glaciers is not gained by aquifers or lakes.

8.4. MODELLING TOOLS

8.4.1. Volume–Area Scaling

Sustained mass loss implies shrinkage of the glacier, reduction of its thickness, and eventual disappearance. Given measured or modelled rates of mass loss, and initial thickness (with a reasonable assumption about bulk density), the mass loss, shrinkage, and thinning can be tracked by simple book-keeping, for which the most frequently used tool is volume–area scaling.

Volume–area scaling is glaciological jargon for the observed tendency of glacier volume to be proportional to glacier area. It is a misnomer, because the independent quantity that is found to be proportional to area is mean thickness (Figure 8.5). Objections to the statistical propriety of correlating area with volume, because volume is the product of mean thickness and area, are therefore without merit. In volume–area scaling, a two- or sometimes three-parameter relationship is fitted to measurements of mean thickness and area. There are, however, at most a few hundred such measurement pairs, although the

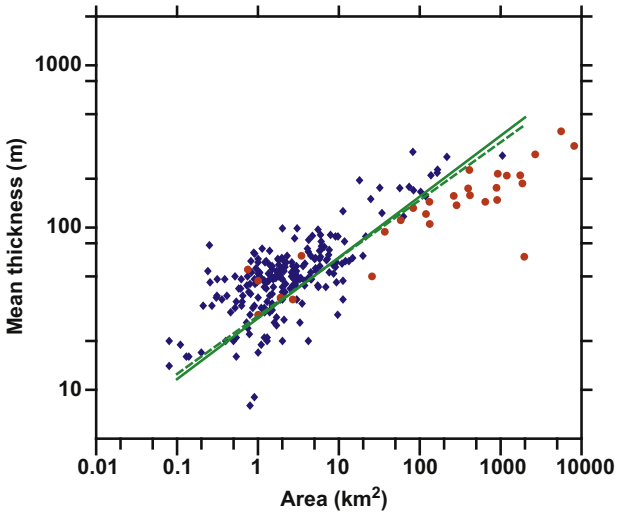

FIGURE 8.5 Measured mean glacier thickness as a function of glacier area for a compilation from the literature of 226 valley and mountain glaciers (diamonds) and 30 ice caps (circles). The most commonly employed scaling relationships are shown as lines (dashed: Chen and Ohmura, 1990; solid: Bahr et al., 1997); they were derived from smaller samples ($n = 61$ for Chen and Ohmura; $n = 144$ for Bahr et al.) excluding ice caps, for which a different scaling is appropriate.

area is known and tabulated for more than 10^5 glaciers. Scaling relationships such as those seen in Figure 8.5 have, thus, become the basis for estimating the volume and mass of glaciers whose thickness has not been measured.

Bahr et al. (1997) offer an elegant argument, finding that mean thickness ought to be proportional to the 3/8ths power of area. Measured mean thicknesses, H, are well-described by a relation with area, S, of the form:

$$H = cS^{\beta} \tag{8.5}$$

which is the basis for the volume–area relation:

$$V = S\,H = cS^{\gamma} \tag{8.6}$$

in which $\gamma = 1 + \beta$, and c and β are the fitted parameters. There is good evidence that estimates of the exponent β from observations, near to 0.36 (see also Chen and Ohmura, 1990), are consistent with the theoretical expectation, although the factor c appears to be more variable.

Equation (8.5) can be inverted. Suppose that a known mean thickness H changes by a known amount ΔH:

$$H_* = H + \Delta H \tag{8.7}$$

We can write:

$$S_* = (H_*/c)^{1/\beta} \tag{8.8}$$

for the new area S_* implied by the thickness change and the parameter set (c, β). If $\Delta H < -H$, the glacier disappears. ΔH itself is obtained from the measured or modelled mass balance ΔM as:

$$\Delta H = \Delta M/\rho \tag{8.9}$$

where $\rho = 900$ kg m^{-3} is the density usually assumed for the glacier.

One limitation of scaling relations such as Equation (8.5) is their simplicity. Glaciers of the same area can vary greatly in thickness (Figure 8.5) and other ways of parameterizing mean thickness have been proposed. For example, Haeberli and Hoelzle (1995) related thickness to the surface slope and the basal shear stress, itself parameterized in terms of the elevation range of the glacier. Although there are good dynamical reasons for expecting such a relationship, the observational support, traceable to Maisch and Haeberli (1982), is not strong. A fruitful practical approach would be to estimate thickness with a multivariate relationship, but this has not yet been attempted.

8.4.2. Temperature-Index Models

Temperature-index models are models of mass balance in which surface ablation is estimated as a function of temperature, often near-surface air temperature measured either on the glacier or at the nearest weather station. Temperatures may also be taken from upper-air soundings, meteorological datasets (as in the promising recent work of Hirabayashi et al., 2010), or climate models. Most often, the chosen index of temperature is the positive degree-day sum.

The positive degree-day sum, φ, over any timespan is the integral of the excess of temperature, T, above the melting point, T_m:

$$\varphi = \int_{t_1}^{t_2} \max[0, T(t) - T_m]\ dt \tag{8.10}$$

In practice, $T(t)$ is available as a series of averages over some time step, or instantaneous values at some interval, of near-surface air temperature, T_i ($i = 1, \ldots, n$), and the expression, with T_i in degrees Celsius, becomes:

$$\varphi = \Delta t \sum_{i=1}^{n} \max[0, T_i] \tag{8.11}$$

where Δt is expressed in days. The ablation, a, by melting and sublimation over the span, at a point on the glacier surface, is assumed to be linearly proportional to φ:

$$a = -f\varphi \tag{8.12}$$

(By glaciological convention, lower-case letters are used for mass-balance components of parts of a glacier, while upper-case letters are used for the whole glacier or for collections of glaciers.) The degree-day factor, f, is a parameterization, and therefore a simplification, of the energy balance. It is usually treated as one or more constants. Hock (2003) has reviewed published determinations of the degree-day factor (Figure 8.6). The median for snow is 4.5 kg m^{-2} (K d)$^{-1}$ and for ice it is 7.6 kg m^{-2} (K d)$^{-1}$, greater by a factor

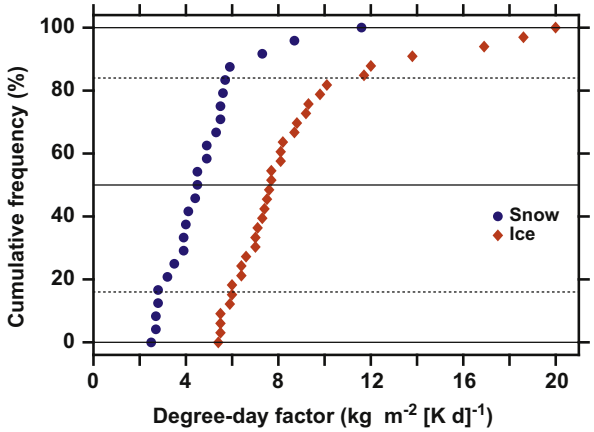

FIGURE 8.6 Degree-day factors for snow and ice estimated from field measurements and summarized in table 1 of Hock (2003). The median (50th percentile) of the cumulative frequency distribution is shown as a solid horizontal line and the 16th and 84th percentiles are shown dotted.

of 1.7. The strongly skewed upper tail of the distributions in Figure 8.6 represents measurements in Greenland, Svalbard, Switzerland, and the Himalaya, and the reasons for it appear to be diverse and not well understood. The body of the distribution, below the 84th percentile, is almost linear for both snow and ice. Its range on the f axis, about 3 and about 5 kg m^{-2} (K d)$^{-1}$ for snow and ice respectively, can be conjectured to reflect, for 'normal' circumstances, a combination of measurement uncertainty and the extent to which the temperature-index approach simplifies the energy balance.

Ohmura (2001) has explained the success of temperature-index models. During the ablation season, the glacier surface is at the melting temperature, the near-surface air is warmer than the surface and the sensible heat flux (Section 8.2.3) is directed downwards. However, Ohmura stressed the role, firstly, of the atmospheric infrared radiation as an energy source for ablation and, secondly, of the near-surface air temperature as a predictor of the atmospheric radiation, much of which comes from the lowest 1 km of the atmosphere. The near-surface air temperature can thus be a very good predictor of the largest energy source for ablation and can also be strongly correlated with the sensible heat flux. There is also usually a correlation with the solar irradiance. Sicart et al. (2008), however, present counter-examples to all of these generalizations, noting that, although atmospheric radiation is indeed the main energy source in most cases, it tends to vary little and its variations are due mainly to variations in cloud cover.

In the context of glaciological modelling, temperature-index models are valuable because temperatures are among the most widely available of climate model outputs, and their attributes, including their defects, have been analysed intensively. The temperature-index models go far towards solving the problem of coupling climatic forcing, at large spatial scales, to the response of the glaciers, all of which are smaller than a GCM grid cell. (The two ice sheets are special cases.) There are residual problems, the greatest of which is that climate model topography is smooth but the glaciers have large vertical ranges. The solution adopted for this problem (e.g., Radić and Hock, 2011) is to apply a suitable lapse rate, and usually also a bias correction, to climate model surface temperatures. Sometimes, the climate model's free-air temperatures are interpolated to glacier surface elevations.

Glacier models that rely on climate models for forcing normally derive accumulation from the climate model precipitation. The fraction of precipitation that is snow is estimated as a function of interpolated temperature. Sometimes, a lapse rate of precipitation is also implemented, although the tendency of precipitation to increase with elevation is less well-constrained either by physical understanding or by observations.

8.4.3. Energy-Balance Models

Hock (1999) showed that the performance of a temperature-index model improved significantly when a radiative term and a correction for shading by topography were introduced. This model is representative of several that are intermediate in complexity between the simple, but sufficiently successful, temperature-index models and fully-fledged energy-balance models that solve Equation (8.2) explicitly. Energy-balance models, however, are more demanding than temperature-index models and are not often used in long or large-scale simulations. The minimum of additional required information beyond near-surface air temperature includes net radiation, wind speed, humidity, and vertically-resolved subsurface temperature.

All modern GCMs, of course, have land-surface schemes that compute the components of Equation (8.2). The difficulty is that the glaciers are not resolvable at the scale of a GCM grid cell. The GCMs cannot resolve the strong dependence, $\partial a/\partial z$, in specific units, of the ablation on elevation (Figure 8.1), nor can they resolve the widespread tendency for $\partial c/\partial z$ to be significant, that is, for accumulation to be greater at higher elevations; hence, the need for off-line calculations of the glacier response to climatic forcing.

Bougamont et al. (2007) provide a cautionary example of the possible limitations of the temperature-index approach. Comparing a positive degree-day model and an energy-balance model of the surface mass balance of the Greenland Ice Sheet, they find that the positive degree-day model produces almost twice as much meltwater runoff as the energy-balance model. Much of the difference is due to the more detailed simulation of subsurface temperature, and consequently the greater refreezing, in the energy-balance model. In the near absence of observational support, however, it is difficult to judge between the different parameterizations of refreezing.

8.4.4. Mass-Balance Sensitivity

Changes in the climatic mass balance, B, can be understood in terms of sensitivity to both temperature and precipitation. It is always found (e.g., Oerlemans and Reichert, 2000) that at a given location the sensitivity to precipitation, $\partial B/\partial P_r$, where $P_r = P/P_{ref}$ is the actual precipitation normalized by the precipitation of some reference period, contributes less to change in B than does the sensitivity to temperature, $\partial B/\partial T$. Also, it is generally found that there is a non-zero sensitivity of precipitation to temperature, the climate growing wetter as it grows warmer.

The sensitivity to temperature is a close relative of the degree-day factor, f, discussed above (Equation (8.12)), but it is important to be aware that $\partial B/\partial T$ is estimated sometimes from the output of temperature-index or

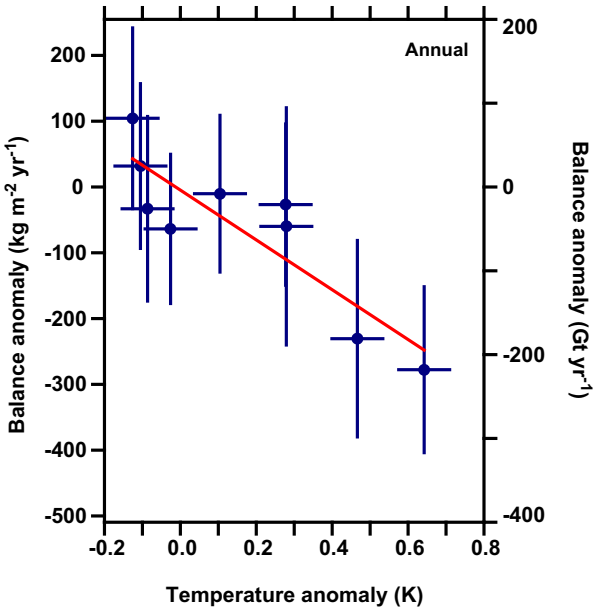

FIGURE 8.7 Correlation of the anomaly (relative to the 1961–1990 average) in pentadal (5-yearly) mean annual climatic mass balance, B, (Kaser et al., 2006) with the corresponding anomaly in T, surface air temperature over land (CRUTEM3; Trenberth et al., 2007). With 2-standard-error uncertainties, the fitted line suggests a proportionality $\partial B/\partial T$ of -379 ± 170 kg m^{-2} yr^{-1} K^{-1} or (with the Kaser et al. area of 0.785 Mm^2) -297 ± 133 Gt yr^{-1} K^{-1} for the era of glaciological balance measurements (1960/61–2003/04). *(Source: Steffen et al., 2008, with permission.)*

energy-balance models and sometimes from a comparison of measurements of B and T. In the latter case, changes in variables other than temperature are often neglected as possible causal agents. Furthermore, at large (for example, global) spatial scales the sensitivity may be estimated over a reference period, as in Figure 8.7, but is unlikely to remain unchanged over a longer simulation period. One reason is that the simulated B will be an integral over a varying, usually a diminishing, total glacierized area. In Figure 8.7, even the shrinkage of the glaciers over the 45-year reference period has been neglected, for lack of adequate information. Nevertheless, sensitivities estimated for the recent past do tend to agree well. Raper and Braithwaite (2006) and Meehl et al. (2007) quote a total of six sensitivities to global temperature that were obtained in diverse ways. They range from -320 to -410 kg m^{-2} yr^{-1} K^{-1}, with an average of -373 kg m^{-2} yr^{-1} K^{-1} that is almost identical to the sensitivity of Figure 8.7.

8.4.5. Models of Glacier Dynamics

Over decades or longer spans of time, detailed simulations of glacier evolution require accurate simulation not just of the energy and mass balances, but also of the force balance. There are subtle links between the force balance and the mass balance, because the ice flows from where there is net accumulation to where there is net ablation, although the interplay is governed by glacier size and by the timescale of glacier motion. Typical resulting timescales (Greve and Blatter, 2009) are 10^2 years for a medium-sized valley glacier, 5×10^2 years for an ice shelf and 10^4 years for an ice sheet.

The force balance is not treated here; see, for example, Cuffey and Paterson (2010) for a standard development. At present, the much longer glaciological timescales rule out any direct computational coupling between glacier-dynamics models and climate models that take time steps of the order of 30 minutes. One critical dynamical problem, the mismatch between the ice-shelf and ice-sheet timescales, or more generally the floating-ice and grounded-ice timescales (Section 8.7.2), is responsible in large part for the present lack of trustworthy projections of ice-sheet responses to twenty-first century climatic forcing.

Volume–area scaling and temperature-index modelling of the mass balance lead, when taken together, to coherent responses of glacier size to glacio-climatic forcing. On the whole, they appear to be reasonably successful substitutes for detailed simulation of the force balance. Nevertheless, relatively simple models of glacier dynamics (Oerlemans, 2001) are also available and offer valuable insight, not limited to the validation of yet simpler models. For example, Reichert et al. (2002) coupled a mass-balance model and an ice-flow model to study two European glaciers that have long records of length fluctuations. The mass-balance model was coupled via seasonal mass-balance sensitivities to GCM output from a control simulation in which external forcing (solar, volcanic, and anthropogenic) was excluded, leaving only internal climatic variability. They demonstrated that the observed acceleration of retreat during the twentieth century is a highly improbable response to internal variability.

8.5. RECENT AND PRESENT STATES OF THE WORLD'S GLACIERS

8.5.1. Kinds of Change

Broadly speaking there are four ways in which we can measure glacier changes. In the climate of recent centuries, nearly all glaciers have been getting smaller, and the sign of the changes is not expected to change in the foreseeable future.

- *Retreat*: Retreat is reduction of the glacier's length. It is easy to measure, so there are many measurements, and difficult to relate to other measures of change (but see Section 8.5.2).
- *Shrinkage*: Shrinkage is reduction of the glacier's area. It requires a measurement effort greater than that for

retreat, but the measurements can be made readily by airborne and particularly satellite remote sensing. Discriminating glaciers from seasonal snow, and debris-covered ice from ice-free terrain, presents difficulties, but the quantity and information content of shrinkage measurements are growing steadily.

- *Volume change*: To measure volume change, measurements are required of the change not just of area, but also of mean thickness. Accurate geodetic measurement of thinning is challenging, but is contributing in increasing quantity and value to our understanding of the recent evolution of glaciers.
- *Mass balance*: The preferred measure of change in most contexts is the mass balance. The change of mass can be estimated from the change of volume if a suitable density can be assumed for the mass gained or lost, but until recent years most measurements of mass balance were made by the glaciological method (Section 8.3.1), which is time-consuming and expensive. Although in situ glaciological measurements cannot match the spatial coverage of geodetic measurements, or the temporal resolution (monthly or better) of gravimetric measurements by the GRACE satellites, they continue to provide the bulk of annually-resolved observational estimates of change.

8.5.2. Evolution of Glacier Mass Balance Since the Little Ice Age

Worldwide observations of glacier terminuses dating from as long ago as the sixteenth century have been compiled by Leclercq et al. (2011). The density of observations is sufficient for detailed analysis only after 1800. Leclercq et al. normalized the glacier length changes and calibrated them against normalized mass changes. The sample of single-glacier length changes is rather coherent when regionalized. It shows stability or terminus advance until the culmination of the Little Ice Age in the mid-nineteenth century, with retreat thereafter in all regions. A well-defined global signal emerges (Figure 8.8) when mass change is scaled to length change with a single glacier-shape parameter. Terminus advance and mass gain become retreat and loss respectively in about 1850. Leclercq et al. estimated the glacier mass loss between 1850 and 2001 (the start date of the regularized projections discussed in Section 8.6.1) as 88 mm $\pm$ 22 mm SLE (Section 8.3.2), at an average rate of about 0.6 mm SLE yr^{-1}. Depending on the total mass estimated for 2001 (Section 8.6.1), the implied fractional loss since the culmination of the Little Ice Age is of the order of one eighth or somewhat greater.

Detecting recent change in glacier mass balance is thus the problem of detecting, against a background of natural variability, a shift from a moderate rate of loss, as the cryosphere emerges from the Little Ice Age, to a faster rate of loss, at least if anthropogenic radiative forcing has played its expected role. The problem is difficult at the century timescale of Figure 8.8, in part because, as will be seen in Section 8.5.5, there was a shorter-term relative maximum of mass balance in the 1960s and 1970s.

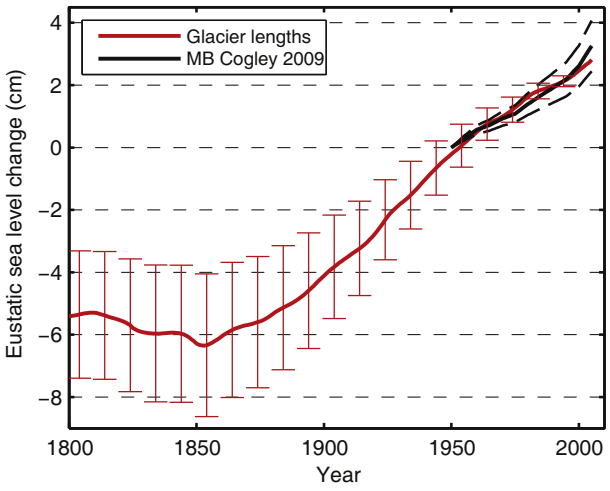

FIGURE 8.8 Reconstruction (red), from a scaling of mass change to length change, of the cumulative small-glacier contribution to sea-level change relative to an arbitrary zero in 1950. The cumulative mass-balance record (black, with upper and lower estimates shown as dashed lines) is from Cogley (2009). *(Source: Reprinted with permission from Leclercq et al., 2011. With kind permission from Springer Science+Business Media.)*

8.5.3. Measurements of Shrinkage

Reasonably accurate glacier outlines have been reconstructed for dates as old as the seventeenth century from terminal moraines and similar relict landforms. The oldest maps of adequate accuracy for the measurement of areas were made in Switzerland in the 1860s. Numerous more recent measurements have been published, but they remain uncompiled, so a quantitative global picture of the magnitude and variability of shrinkage rates is not readily available.

Cogley (2008), however, presented a preliminary compilation of 685 measurements of the shrinkage of single glaciers and 271 measurements of regional shrinkage. In the sample as a whole, typical shrinkage rates in the late twentieth century are -0.10% yr^{-1} to -0.40% yr^{-1} and, for glaciers or regions with two or more measurements (that is, three or more area measurements), it is found more often than not that the shrinkage rate has accelerated. But these generalizations conceal some important sources of variability that are difficult to handle. The most difficult is the strong but not universal tendency for regional rates to vary strongly with initial glacier size. Bigger glaciers are found to shrink at much slower rates. The smallest, and on average fastest-shrinking, glaciers

have highly variable rates. However, some studies document an absence of this size dependence of shrinkage rate, and the size distribution (the frequency distribution of glacier area, as in Figure 8.9a) is not known at all for several extensively glacierized regions, so that any estimate of the globally-averaged rate would be very uncertain.

Such an estimate of the globally-averaged rate of glacier shrinkage would nevertheless be valuable. Apart from their intrinsic value as indicators of environmental change, shrinkage rates are important as the basis for providing more sharply-focused initial conditions for mass-balance projections such as those of Section 8.6.1. Depending on which region is chosen as a pattern, the global shrinkage rate might be $-2500\ \mathrm{km^2\ yr^{-1}}$ (strong size dependence, as exhibited by the European Alps or the Queen Elizabeth Islands of arctic Canada) or it might be only $-500\ \mathrm{km^2\ yr^{-1}}$ (no size dependence, as indicated by some studies in western North America). The initial areas in Table 8.1 derive from inventories spread over several decades in the late twentieth century, and the information cannot be corrected with confidence to the year 2001, or any other year.

The rates just quoted translate to a fractional reduction of extent over 50 years of from less than 5% to as much as 20%. Recently, Dyurgerov (2010), drawing on regional shrinkage rates where available, estimated the global total shrinkage for 1961–2006 as −5.6%, a rate of $-0.13\%\ \mathrm{yr^{-1}}$.

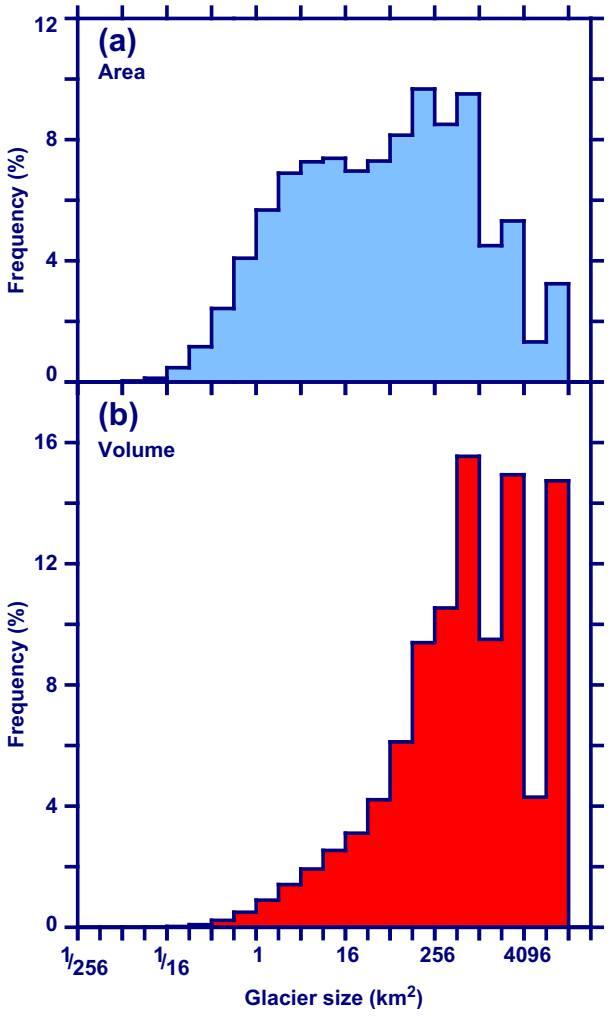

FIGURE 8.9 (a) Frequency distribution of the areas of 129,108 glaciers in the World Glacier Inventory (Cogley, 2009b). Total area covered is 0.343 $\mathrm{Mm^2}$, representing slightly less than half of the total small-glacier area. (b) Areal frequency distribution of glacier volumes, obtained from panel a by volume–area scaling (Equation (8.6)) with the parameters of Bahr et al. (1997).

8.5.4. Present-Day Extent and Thickness

Incomplete as it is, the World Glacier Inventory is the most reliable global source of physiographic information about glaciers. At present, the version containing the most glaciers, currently about 134,000, is that of Cogley (2009b). It accounts for nearly one half of the global extent of small-glacier ice, recording a varying number of attributes for each glacier. The inventory does not include glacier outlines or hypsometric curves explicitly, although glacier outlines are the central feature of the Global Land Ice Measurements from Space initiative (Raup et al., 2007), a resource of growing importance. Hypsometry can be derived readily by using the outlines to mask a digital elevation model, such as the ASTER Global Digital Elevation Model or that of the Shuttle Radar Topography Mission (Hayakawa et al., 2008). The stringent accuracy requirements for measurements of elevation change (Section 8.3.1) can be relaxed for the modelling of glacier–climate relations.

Figure 8.9a shows the frequency distribution of glacier area from the incomplete inventory. This distribution, although it has no value for the estimation of size distributions in regions with missing information, is useful for the purpose of putting glacier changes in perspective. For example, the evolution of glaciers in the present climate and that projected for the twenty-first century implies a shift of the histogram to the left, by the shrinkage and eventual vanishing, and occasionally by the fragmentation, of individual glaciers. That glaciers are vanishing is a journalistic commonplace and a correct observation, but those that have already vanished are those that were never very big in the first place. They probably formed during the Little Ice Age, and at present occupy the smallest-size classes of the histogram. While those classes are not negligible, most of the extent is accounted for by much larger glaciers that will be much longer-lived. The main reason for their expected longevity is seen in Figure 8.9b, which shows that the concentration of volume in larger glaciers is even more marked, by virtue of Equation (8.6), than that of extent.

The most objective estimate of the total area of glaciers outside the ice sheets to have appeared so far, 0.741 mm ± 0.068 Mm^2, is that of Radić and Hock (2010). They generated the global total from the inventory of Cogley (2009b), supplemented by the older work of Cogley (2003) and by a much older estimate for peripheral glaciers in Antarctica. This Antarctic estimate includes the ice rises, bodies of grounded ice within the ice shelves. Nothing is known of their mass balance, but they are mostly at such high latitudes that they experience little or no surface ablation today. In addition to this source of uncertainty, the uncertainty assumed by Radić and Hock, ±10% for most of the glaciers, should be taken seriously. It is an antidote to the temptation to believe that areas are so well-known that errors can be neglected. In fact, the measurements themselves, or more accurately the mapmaking and image interpretation on which they are based, are quite uncertain. Inability to correct for shrinkage over the timespan covered by the measurements (Section 8.5.4) introduces further uncertainty.

Radić and Hock (2010) constructed glacier size distributions for regions without complete inventories by an upscaling procedure. By volume−area scaling they then estimated the total small-glacier mass as 600 mm ± 70 mm SLE (Table 8.1). This is dwarfed by the ice in the two ice sheets. Lythe and Vaughan (2001) estimated the mass of the Antarctic Ice Sheet as 22.6 million Gt, or about 62.5 m SLE. The latter figure becomes about 57 m SLE when ice below sea level is replaced by seawater. The mass of the Greenland Ice Sheet, based on the volume calculated by Bamber et al. (2001), is 2.69 million Gt or, without allowance for a small volume that lies below sea level, 7.4 m SLE.

The corresponding mean thicknesses are 2000 m for the Antarctic Ice Sheet and 1715 m for the Greenland Ice Sheet. The total volume and area of Radić and Hock (2010) yield a mean thickness of 294 m for the other glaciers.

8.5.5. Recent Evolution of Glacier Mass Balance

Measurements of glacier-wide mass balance by geodetic methods go back to the mid-nineteenth century and by glaciological methods to the mid-twentieth century. However, the number and distribution of the measurements is adequate for objective global estimation only since about 1960. Three recent global estimates (Ohmura, 2004; Dyurgerov and Meier, 2005; Cogley, 2005) were synthesized by Kaser et al. (2006) (see also Lemke et al., 2007) into a 'consensus estimate', the term reflecting the broad agreement between its components. The agreement is unsurprising because the component datasets are nearly the same, and the variation between them is due mainly to different treatments of the problem of spatial bias. The measurements come disproportionately from some mountain ranges, while other regions of extensive glacierization contribute few or no measurements.

The most prominent feature of the consensus estimate is a relative maximum of mass balance centred near 1965−1970. The few measurements before 1960 indicate a more negative global average and, although the indications are weak, they are consistent with other lines of evidence (Section 8.5.2). It is clearer that in recent decades the global average has been growing more negative, although not steadily. The relative maximum of the 1960s and 1970s coincides with an episode of cooling, or slower warming, that is well-documented in temperature records (e.g., Jones and Moberg, 2003), and this coincidence underpins and quantifies (Figure 8.7) the concept of mass-balance sensitivity to temperature.

The most recent global estimates are those of Dyurgerov (2010) and Cogley (2009a). The Dyurgerov estimate is the first to allow explicitly for glacier shrinkage, which makes the global-average total balance less negative, although only moderately so, as time passes. The Cogley (2009a) estimate, summarized in Figure 8.10, resembles the Kaser et al. (2006) estimate, but there is at least one important new detail. In Figure 8.10a, the pentadal estimates are simple unweighted arithmetic averages of the available measurements. The blue circles are averages of geodetic measurements, newly compiled and used for the first time in a global assessment. They provide greater historical depth than the glaciological measurements (red squares) and suggest that the relative maximum at about 1965−1970 was a modest affair. (In the figure, the maximum appears as a minimum because mass balance and sea-level rise are of opposite sign.) More significantly, the balance averages are consistently more negative than the glaciological estimates. Considering that calving glaciers are better represented in the geodetic dataset, the most likely explanation, which has not yet been tested in detail, is that calving glaciers have more negative mass balances. In any case, including the geodetic measurements makes a substantial difference.

Figure 8.10b is the result of a detailed exercise in polynomial spatial interpolation, the aim of which is to correct the uneven representation of glacierized regions in the datasets. It extends back only to the 1950s because the measurements are too few for interpolation at earlier dates. The shapes of the two spatially-corrected histories are similar, but the offset seen in Figure 8.10a survives. (The dark blue circles are actually based on all measurements, combining the glaciological and geodetic datasets, as described by Cogley (2009a).) However, the spatial correction makes the average balances significantly less negative because regions suffering relatively moderate losses are under-represented in the data.

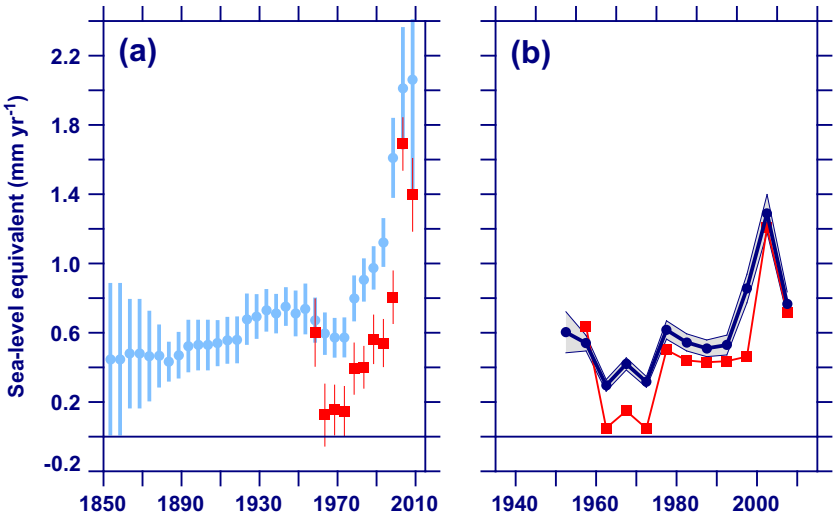

FIGURE 8.10 (a) Pentadal (5-yearly) arithmetic averages of all geodetic (blue circles) and glaciological (red squares) small-glacier mass-balance measurements, 1850–2010. Data updated from Cogley (2009a). Vertical bars represent ±2 standard errors about the mean. (b) Pentadal global averages of mass balance for 1950–2010 estimated with a correction for spatial bias of the datasets as in Cogley (2009a). Red squares rely only on glaciological measurements; dark blue circles with grey confidence envelope (2 standard errors) rely on both glaciological and geodetic measurements. The most recent pentad is incomplete; most reports for the 2009/10 balance year are not yet available.

The pentadal resolution of Figure 8.10 is chosen so as to increase statistical confidence, detrended annual mass balances being serially uncorrelated. However, it also maintains the independence of successive terms in the series while suppressing much of the inter-annual variability and, thus, showing that there is considerable variability in glacier mass balance at decadal scales. In particular, the very negative balances of the early 2000s have not been sustained in the most recent pentad, 2005/06–2009/10, in which glaciers have experienced more moderate although still large losses. This decadal variability means that projections of the simple if-present-trends-continue kind ought to be assessed with caution, at least to the extent of noting carefully the definition of 'present'.

In terms of the energy balance, the mass balance for the pentad of most rapid loss, 2000/01–2004/05, consumed about 6.7 W m^{-2} over the glacierized area, while the 36.4 mm SLE of loss over 1950/51–2008/09 consumed about 3.2 W m^{-2}. As components of the energy balance of the entire Earth, these fluxes are equivalent to 0.010 and 0.005 W m^{-2} respectively, and are small with respect to, for example, the ~0.2 W m^{-2} by which the ocean has been heated during 1950–2009 (Murphy et al., 2009; Sen Gupta and McNeil, 2012, this volume).

Technological advances in radar interferometry; radar and especially laser altimetry and, most recently, gravimetry have made measurements of the mass balances of the ice sheets a reality in the past 20 years. Syntheses with good temporal resolution have been made possible by advances in meso-scale meteorological modelling, which can now provide accurate simulations of accumulation, as well as in the parameterization (Section 8.4.2) or modelling (Section 8.4.3) of the surface energy balance to yield reliable estimates of melting and sublimation. The most recent assessment of ice sheet mass balance (Rignot et al., 2011) is summarized in Figure 8.11. The climatic mass balance is simulated by a meso-scale climate model and the calving flux at the grounding line is obtained from interferometric measurements of velocity, measurements of ice thickness by radio echo-sounding, and an allowance for migration of the grounding lines of some of the largest outlet glaciers.

There is substantial inter-annual variability in the ice sheet balance series, but Rignot et al. (2011) estimate accelerations during 1992–2009 of −21.9 Gt ± 1.0 Gt yr^{-2} for the Greenland Ice Sheet and −14.5 Gt ± 2.0 Gt yr^{-2} for

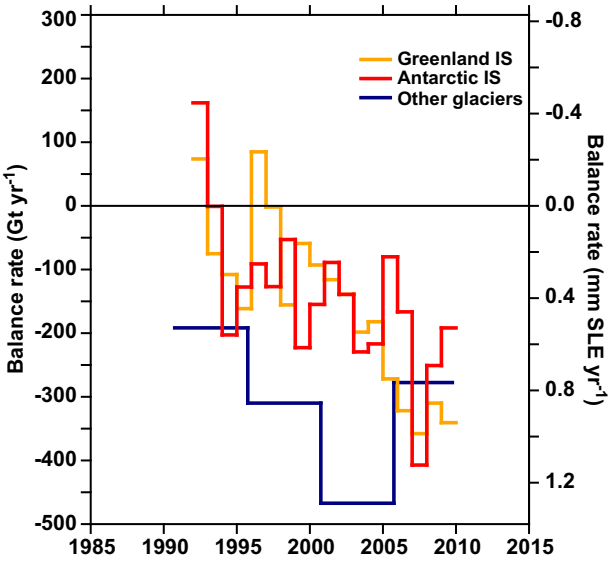

FIGURE 8.11 Annual mass-balance rate, 1992–2009, of the two ice sheets (calendar-year averages of monthly balances from figure 2 of Rignot et al. (2011)), and pentadal mass-balance rate (balance years 1990/91–2008/09) of all other glaciers (from Figure 8.10).

the Antarctic Ice Sheet. For comparison, a trend fitted to the small-glacier balance rates for 1970/71–2008/09 in Figure 8.10 yields an acceleration of −8.0 Gt ± 0.4 Gt yr^{-2}. The recent moderation of losses from the other glaciers means that the three reservoirs of ice have contributed to sea-level rise at comparable rates over 2006–2009, with the Greenland Ice Sheet contributing the most. The sum of the three contributions for 2006–2009 is −854 Gt yr^{-1} or 2.4 mm SLE yr^{-1}.

8.6. THE OUTLOOK FOR GLACIERS

8.6.1. Future Contributions to Sea-Level Rise

Table 8.1 and Figure 8.12 form the centrepiece of this study, summarizing the principal recent estimates of the global evolution of glaciers over the twenty-first century. The estimates are diverse in methodology. They range from detailed modelling of glacier response to modelled climatic forcing to estimates based on glacier physiography and on expert judgement.

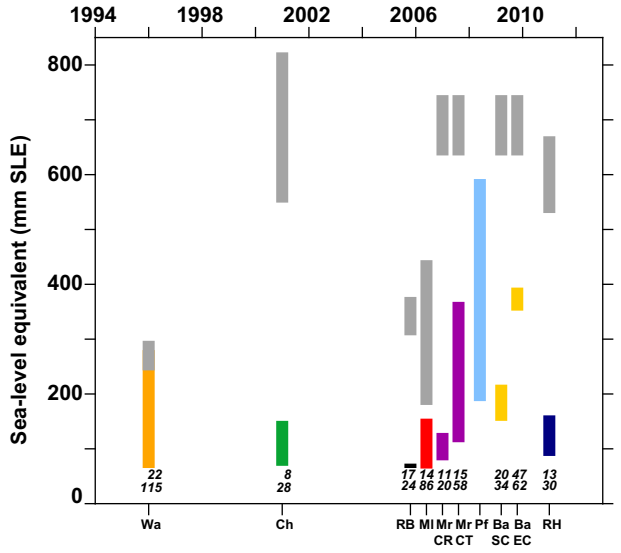

FIGURE 8.12 Regularized projections of sea-level rise ('Final SLR', in colour) due to small-glacier mass balance from 2001 to 2100. Bar height represents range of estimates; bar width is arbitrary. See also Table 8.1. Above each projection (except for Pf) is a grey bar representing Initial mass. Below each projection is given the range of projected ratios of 'Final SLR' to 'Initial mass', as percentages. (That is, the upper and lower numbers are respectively the ratios of the bottom of the coloured bar to the top of the grey bar and of the top of the coloured bar to the bottom of the grey bar.) Tick labels on vertical axis, if divided by 100, give the twenty-first century average rate of rise in mm SLE yr^{-1}. *(Sources: Wa (orange) – Warrick et al., 1996; Ch (green) – Church et al., 2001; RB (black) – Raper and Braithwaite, 2006; Ml (red) – Meehl et al., 2007; MrCR (purple) – Meier et al., 2007, constant rate; MrCT (purple) – Meier et al., 2007, constant trend; Pf (light blue) – Pfeffer et al., 2008; BaSC (yellow) – Bahr et al., 2009, steady climate; BaEC (yellow) – Bahr et al., 2009, evolving climate; RH (dark blue) – Radić and Hock, 2011.)*

In an attempt to eliminate variations that arise from discrepancies of technical detail, the projections of 'Final SLR' (cumulative sea-level rise, 2001–2100) have been 'regularized'. That is, where the authors' original projections were for different durations, they were multiplied by suitable factors near to 1.0 to yield estimates for a span of 100 years. In two cases (Church et al., 2001; Raper and Braithwaite, 2006), the projections were multiplied by equally crude ratios of glacierized areas so as to account for omission of the poorly-known peripheral glaciers in Greenland and Antarctica. Where confidence envelopes for Final SLR were presented as standard errors, and, in some cases, as standard deviations, they have been converted to ranges. Although some of the confidence envelopes were derived from end-to-end error analyses of the corresponding calculations, none of the calculations address all of the known sources of uncertainty, and so none of the confidence envelopes can lay claim to statistical completeness.

It is important, therefore, to realize that the results displayed here may depart from the authors' original intentions, although the regularization does enhance the comparability of the items of information.

The initial areas given in the sources have not been regularized in Table 8.1, and their uncertainty, which is substantial, has not been tabulated. The surveys and maps on which they are based are spread over several decades of the late twentieth century, with some regions having no adequate maps. There is, as yet, no clear picture of how regional shrinkage rates have evolved and it is not practicable to correct the areas objectively so that they represent a single year, such as 2001. The largest source of uncertainty, lack of knowledge of the glaciers peripheral to the two ice sheets, has been addressed in the regularization described above but, although estimates of their area are not very accurate, their mass-balance rates are even more poorly known. A particular ambiguity arises from the inclusion of peripheral glaciers in Antarctica, where the initial area may or may not include the ice rises (Section 8.5.4).

The specific balance rate in Table 8.1 is described as 'notional' because it represents ablation over 100 years divided by the glacierized area at the start of the interval. The area is certain to continue to decrease over the interval and actual balance rates per unit of surviving area will be more negative at each time during the interval. The notional rate, however, is useful as a rough guide to the intensity of mass loss.

8.6.1.1. IPCC Assessment Report 2

Warrick et al. (1996) estimated sea-level rise due to glacier mass balance with a model (Wigley and Raper, 1995) in which glaciers within a number of regions evolve, with a common regional response time, under forcing that is

TABLE 8.1 Regularized Projections of Mass Loss from Small Glaciers Between 2001 and 2100

Source	Initial Area (Mm^2)	Initial Mass (mm SLE)	Final SLR (mm SLE)	Notional Balance Rate[a] ($kg\ m^{-2}\ yr^{-1}$)	Remarks
Warrick et al., 1996[b] (IPCC SAR[c])	0.680	~270	65 – 280	−346 to −1493	Sensitivity of ice mass to temperature change; range of 3 projections under the IS92a scenario
Church et al., 2001[d] (IPCC TAR[c])	0.540	686 ± 137	69 – 151	−336 to −738	Sensitivity of mass balance to temperature, and volume–area scaling; range of 9 GCMs, IS92a scenario
Raper and Braithwaite, 2006[e]	0.522	342 ± 35	65 – 73	−430 to −480	Degree-day model, triangular hypsometric curve; A1B scenario, 2 GCMs
Meehl et al., 2007[f] (IPCC AR4[c])	0.512–0.546	180 – 444	64 – 155	−440 to −1066	Simple climate model, 6 SRES scenarios
Meier et al., 2007	0.763	690 ± 55	79 – 129	−375 to −645	Constant mass-balance rate
Meier et al., 2007	0.763	690 ± 55	112 – 368	−560 to −1840	Constant mass-balance trend
Pfeffer et al., 2008	n/a[g]	n/a	187 – 592	n/a	Deliberate search for an upper bound, involving expert judgement
Bahr et al., 2009	0.763	690 ± 55	151 – 217	−755 to −1085	Glaciers seek equilibrium with projected steady climate of 2006
Bahr et al., 2009	0.763	690 ± 55	352 – 394	−1760 to −1970	Glaciers seek equilibrium with evolving climate
Radić and Hock, 2011[h]	0.741	600 ± 70	87 – 161	−426 to −788	Degree-day model, triangular hypsometric curve; detailed sensitivity analysis; A1B scenario, 10 GCMs

[a]Final SLR (before regularization) converted to (negative) kg and divided by the product of initial area and the duration of the projection.
[b]Initial area from their table 7.1. Initial mass was assumed to have been 300 mm SLE in 1880; SLR was modelled as ~ 30 mm SLE from 1880 to 2001. Range of Final SLR obtained by multiplying the 2001–2100 SLR of their figure 7.8 by ratios of projections from their figure 7.7.
[c]'ARs': SAR, TAR & AR4 are the Second, Third & Fourth Assessment Report.
[d]Initial mass and Final SLR multiplied by 1.37 = 0.741/0.540 to account roughly for omission of glaciers in Greenland and Antarctica.
[e]Initial mass is the estimate of Raper and Braithwaite (2005a) multiplied by 1.42 = 0.741/0.522 to account roughly for omission of glaciers in Greenland and Antarctica. The source's estimate of Final SLR has also been multiplied by 1.42.
[f]Initial area and mass from Lemke et al. 2007 (table 4.3, rows 1–3), but their initial mass multiplied by 1.20 for consistency with their treatment of glaciers in Greenland and Antarctica. Final SLR from their table 10.7. Average of 3 initial areas used in calculating notional balance rate.
[g]'n/a': not available.
[h]Initial area and Initial mass from Radić and Hock (2010).

parameterized in terms of a temperature change required to raise the equilibrium line to the top of the glacier. An initial mass is prescribed, although the model's initial mass is inconsistent with the estimate of 500 mm ± 100 mm SLE tabulated earlier in the same assessment (in its table 7.1). The high end of the range in Figure 8.12 would require removal of more than the model's initial mass, but it was obtained in the present work, indirectly. Warrick et al. (1996) give a Final SLR for glaciers only for the middle of three IS92a projections, and the range as presented here was obtained crudely by scaling the Final SLR by the ratio of low-to-middle and high-to-middle projections of the sea-level rise from all sources. The Final SLR due to the glaciers in the middle projection is 160 mm SLE.

8.6.1.2. IPCC Assessment Report 3

Church et al. (2001) modelled sea-level change from 1990 to 2090 by the methods of van de Wal and Wild (2001). Temperature projections were taken from nine GCMs running under the IS92a emissions scenario. The sensitivity of mass balance to temperature and precipitation can be traced, apparently, to the results of degree-day and energy-balance modelling of the Greenland Ice Sheet. Changes of precipitation were neglected. Glacierized areas were allowed to evolve by volume–area scaling, with separate estimates for each of 15 glacier size classes in 100 regions. The shrinking extent yielded a Final SLR about 25% less than that obtained with the area held constant.

The Church et al. (2001) Final SLR in Table 8.1, 69 mm–151 mm SLE, is the range of results derived from experiments from nine GCMs but, in a different table, Church et al. present a range of 14 mm–315 mm SLE. (These two ranges are regularized as in footnote d of Table 8.1.) The broader range is the envelope of the 2-standard-error confidence regions surrounding each of eight of the experimental results (J.A. Church and J.M. Gregory, pers. comm.; a standard error of 40% was assumed). The minimum rises on which the low end of the broader range is based are all 30 mm SLE or less and, with one exception, all have been overtaken by events: the actual contribution to sea-level rise from 1990/91 to 2008/09 was nearly 20 mm SLE. Thus, the narrower of the two ranges appears in Table 8.1 because it seems more plausible.

8.6.1.3. Raper and Braithwaite (2006)

Raper and Braithwaite (2006) relied, where possible, on the World Glacier Inventory. Working with temperatures from two GCMs and a $1^\circ \times 1^\circ$ grid of glacierized areas, they applied a degree-day model to ideal glaciers of known vertical extent. The glacier ELAs were adjusted, year by year, in accordance with the GCM temperature change. The degree-day model was used to calculate the mass balance, which, in turn, was used to calculate volume change, area change and change in the area–altitude distribution. The area–altitude distribution of each glacier was assumed to be triangular between its minimum and maximum altitude. Ice caps were considered separately, being assumed to have parabolic profiles. Where the glacier inventory was lacking or incomplete, Raper and Braithwaite (2006) extrapolated from better-known grid cells using a relationship between annual precipitation, summer temperature, and the vertical gradient of modelled mass balance. Thus, the model as a whole stepped through time in response to climatic forcing, with allowance for the dynamical response of the glaciers.

The Raper and Braithwaite (2006) projections are the lowest in Table 8.1. Comparison of their modelling procedure with those of others does not offer an obvious explanation, but it is striking that their estimate of 'Initial mass' (Raper and Braithwaite, 2005a) is well below that of most others. The starting point for their calculation is an old gridded dataset (Cogley, 2003) that was compiled by sparse sampling of small-scale maps, but the probable omission of smaller glaciers implied by the sampling method is unlikely to translate into a large discrepancy with other estimates of glacier volume. The smaller glaciers typically account for only small proportions of regional size distributions and yet smaller proportions of volume distributions, as in Figure 8.9. The lack of reliable glacier size distributions was addressed by modelling well-known regional size distributions in terms of topographic roughness, the latter obtained from TOPO30, a digital elevation model with 30 arc second horizontal resolution (~1 km at the Equator). There is no obvious flaw in their treatment of this relationship and its uncertainty, but it is not possible to validate it empirically outside the seven regions with reliable distributions, so a substantial under-representation on average of large valley glaciers remains a possible explanation (Meier et al., 2005), as was acknowledged by Raper and Braithwaite (2005b). Given the regional size distributions, the scaling by which Raper and Braithwaite (2006) proceed to estimate volumes is a widely-used method (Chen and Ohmura, 1990; Bahr et al., 1997). It seems improbable as an explanation of their low Initial mass, and indeed it is the basis of some of the other estimates in Table 8.1.

8.6.1.4. IPCC Assessment Report 4

Meehl et al. (2007) presented sea-level projections as ranges, which they characterized as "5% to 95% intervals", but acknowledged that they were in fact unable to assess likelihoods because of poorly known uncertainties. The projections were based on a simple climate model (updated from Wigley and Raper, 1992). The global sensitivity of mass balance to temperature was taken to be 0.8 mm ± 0.2 mm SLE yr^{-1} K^{-1}. Meehl et al. (2007) excluded Greenland

and Antarctic glaciers, but multiplied their results by 1.20 to allow for the exclusion. This factor may not be implausible, but it is below the ratio of total glacierized area to the area excluding the Greenland and Antarctic glaciers, which is variously estimated as between 1.30 and 1.45. The factor 1.20 therefore implies that the Greenland and Antarctic glaciers lose mass at less than the global average rate.

The Meehl et al. (2007) ranges may be better regarded as conservative estimates, more 1-sigma-like than 2-sigma-like and therefore more directly comparable with the ranges of the other estimates in Table 8.1. The ranges vary little between the six emissions scenarios from which the climatic forcing was taken. The intense fossil-fuel consumption of scenario A1FI leads to a range of 80 mm−170 mm SLE in Final SLR, while for the middle-of-the-road A1B scenario the range is 80 mm−150 mm SLE and for scenario B1 it is 70 mm−150 mm SLE. Cumulative sea-level rise varies little across the scenarios until the second half of the twenty-first century.

Like that of Raper and Braithwaite (2005a), the Initial mass of Meehl et al. (2007) is relatively low. There were in fact three Initial masses, each deemed equally likely, although it is not clear how the equal likelihood was implemented. One was that of Raper and Braithwaite (2005a), discussed above. The others were from Ohmura (2004) and Dyurgerov and Meier (2005). The Dyurgerov−Meier estimate, 370 mm SLE for glaciers outside Greenland and Antarctica, is closer to other recent determinations. However, the Ohmura estimate, 150 mm SLE for glaciers outside Greenland and Antarctica, is very low. Two thirds of the regional volumes are stated to come from a source that does not, in fact, tabulate volumes, and the largest of the regional estimates, for the Canadian Arctic, is from an early source and cannot be based on full inventory information. In the absence of documentation of the methods, this low estimate must be regarded as doubtful. Noting that a more recent assessment by volume−area scaling (Radić and Hock, 2010) found 193 mm SLE in the incomplete World Glacier Inventory, the Ohmura (2004) estimate can in fact be set aside.

8.6.1.5. Meier et al. (2007)

Meier et al. (2007) argued that, although they account for only about 1% of the total glacier reservoir (about 70 m SLE; Section 8.5.4), glaciers other than the ice sheets can be expected to dominate the cryospheric contribution to sea-level rise between now and 2100. Their estimates of Final SLR are very simple, resting on observations of the recent mass-balance rate and extrapolation to 2100 on two assumptions. Under the constant-rate assumption, the 1995/96−2004/05 balance rate, which they estimate at -527 ± 125 kg m^{-2} yr^{-1} or 1.1 ± 0.24 mm SLE yr^{-1}, is held constant to 2100. Under the constant-trend assumption, the estimated 1995/96−2004/05 trend of -15.6 ± 7.4 kg m^{-2} yr^{-1} is projected to be maintained until 2100.

The constant-rate assumption is likely to be very conservative if warming continues, because there is no reason to expect substantial weakening of the correlation of mass balance with temperature. The constant-trend assumption could perhaps be criticized for its simplicity, but a more serious objection is that under both assumptions the shrinkage of the glaciers is neglected. That is, the mass loss in 2100 is estimated to come from the same area of ice as at the beginning of the century. Meier et al. (2007) counter this objection by noting that most of the present-day glacierized area is accounted for by large glaciers, especially high-latitude ice caps, that will not shrink appreciably during the twenty-first century. They also note that under more intense radiative forcing the disappearance of many smaller glaciers in regions that are already warm will tend to be offset by progressively more negative surface mass balances in the coldest polar regions. In particular, meltwater losses from glaciers in southern Antarctica are currently negligible. This latter argument is of doubtful validity, however, because such glaciers are assigned equal weight with other glaciers throughout the span of the projection.

A significant limitation of the Meier et al. (2007) estimates, as of some others in this section, is that they are based on available mass-balance measurements, which under-represent calving glaciers (Section 8.3.1). Adjacent calving and land-terminating glaciers ought not to have very different mass balances, but the timescale of the mass-balance forcing can be much longer when calving is significant (Section 8.7.2), and one cannot be confident that measurements on land-terminating glaciers, on which the dominant term is the surface mass balance, are representative of calving glaciers. There is strong circumstantial evidence, both globally (Cogley, 2009a) and from studies of single glaciers, that calving glaciers have more negative mass balance at present than do land-terminating glaciers.

8.6.1.6. Pfeffer et al. (2008)

The question of differences of mass balance between calving and land-terminating glaciers was addressed by Pfeffer et al. (2008), who were concerned to estimate the plausibility of very large increases of sea level during the twenty-first century. Their main focus was the Greenland Ice Sheet, which is believed to be vulnerable to rapid mass loss by dynamic thinning, that is, accelerated ice discharge from the terminuses of calving outlet glaciers. However, this accelerated frontal ablation is also characteristic of many of the smaller glaciers. The lower Pfeffer et al. (2008) estimate of Final SLR was obtained by allowing the surface

mass-balance rate to accelerate, as observed in recent years, and by assuming that frontal ablation would be in the same ratio to surface mass balance, as estimated for the Greenland Ice Sheet. The higher Pfeffer et al. (2008) estimate results from an assumption that frontal ablation increases by an order of magnitude during the first decade and remains high thereafter. It exceeds some of the lower estimates of initial mass in Table 8.1 and requires ice velocities that have only been observed rarely and for short periods (hours) on surging glaciers. Whether such fast rates of flow could become prevalent is not known. Very large losses from glaciers other than the ice sheets would require unprecedented ice discharges, accounting for 506 of the estimated total 592 mm SLE during 2001–2100. Such losses are believed to be extremely unlikely but are not known to be impossible.

8.6.1.7. Bahr et al. (2009)

Bahr et al. (2009) did not attempt to model the evolution of the glaciers in detail. Instead, they tried to establish a lower bound on mass loss by interpreting observations of the AAR (Section 8.2.1), which is measured or calculated routinely as a part of most measurements of annual mass balance.

It was learned long ago that on most land-terminating glaciers, zero balance corresponds to an AAR, α, in the neighbourhood of 0.5 to 0.7, and it has long been accepted that this represents a regularity of glacier shape that arises from characteristic patterns of variation of accumulation and ablation with altitude. Bahr et al. (2009) re-examined published records and found a best estimate of 0.57 for α_0, the AAR corresponding to zero mass balance. They also found that multi-annual averages of observed α are near to 0.44. This difference is consistent with evidence of predominantly negative mass balance but it also offers a way to estimate how much additional mass the present-day glaciers must lose because they are too big for the present-day climate.

The Bahr et al. (2009) analysis relies on volume–area scaling (Section 8.4.1). If ΔV_0 is the volume change required to bring a glacier of volume, V, and AAR, α, to equilibrium, that is, to an AAR of α_0, then:

$$\Delta V_0 = V\,[(\alpha/\alpha_0)^{\gamma} - 1] \tag{8.13}$$

The result is that glaciers need to shed 26%–27% of their present-day volume if they are to reach a size in equilibrium with the present-day climate. Bahr et al. (2009) address the likelihood that the climate will keep changing by assuming that the observed α will continue to decrease at the rate seen between the 1960s and 1996/97–2005/06. This assumption, rough as it is, leads to an estimate of $\alpha \sim 0.2$ in 2100, so that the glaciers will by then be even further behind the climatic forcing. Projected mass loss over the century is more than twice as great as for the steady-climate assumption.

The Bahr et al. (2009) estimates in Table 8.1 assume that this equilibrium will be reached precisely at the epoch 2100. The steady-climate estimate also assumes that the climate ceased to change in 2006. Both of these assumptions are improbable, but there is valuable insight in the numbers nevertheless. Firstly, a few to several decades is not unreasonable as a typical timescale for the dynamic adjustment of glaciers to mass-balance forcing. Secondly, we can plausibly interpret the excess of the Bahr et al. (2009) losses over, say, that of Radić and Hock (2011) as a residual response to forcing imposed before 2006 and still to be accomplished after 2100. Thirdly, and most importantly, whatever the date at which the Bahr et al. (2009) Final SLR is realized, it quantifies the notion of committed change in the glaciological context. The glaciers will continue to shrink during the twenty-first century simply because they are not now at equilibrium sizes.

8.6.1.8. Radić and Hock (2011)

The documentation of observational and modelling details in the recent study by Radić and Hock (2011) is more complete than in earlier studies. Necessarily, the documentation is often of shortcomings in the observations and of modelling approximations that are required as responses to those shortcomings. The core of their analysis, which is hierarchical, is an elevation-dependent degree-day model of single-glacier mass balance, with simplified hypsometry interpolated between inventoried minimum, midrange, and maximum glacier elevations. The model is driven by monthly temperatures from the ERA-40 reanalysis and precipitation from a climatological dataset. Model parameters, and model performance in general, are first calibrated against elevation-dependent mass-balance data. The tuned parameters are then extrapolated on a multivariate climatic basis to each glacier in an enlarged version of the World Glacier Inventory (Cogley, 2009b), for which the degree-day model is driven by temperature and precipitation for the period 2001–2100 from 10 GCM experiments run under the A1B scenario. As time advances, the glaciers' sizes are changed using volume–area–length scaling, thus allowing both their areas to shrink and their minimum elevations to rise (Radić et al., 2008). The model thus captures the important feedback of terminus retreat, although it neglects the feedback due to surface elevation change. The inventoried glaciers account for about 40% of the worldwide extent of glaciers. Radić and Hock (2011) define 19 large glacierized regions, for 10 of which the inventory is complete and the regional mass balance is the sum of the single-glacier balances. In the other nine regions, the

regional mass balance is obtained by assuming that the ratio of total mass balance between the inventoried glaciers and all glaciers is equal to the ratio of inventoried to total glacierized area. That is, the specific mass balance of the inventoried glaciers is multiplied by the regional glacierized area, the latter obtained from other sources. The global mass balance is the sum of the regional balances.

Although Radić and Hock (2011) is the most detailed projection of the future of glaciers to have appeared to date, with the most detailed treatment of uncertainties, there are some potentially significant omissions. For example, although it affects only the interpretation of the term 'sea-level equivalent', floating ice and ice grounded below sea level, which already displace seawater, are not distinguished from ice grounded above sea level. All meltwater is added immediately to the ocean, thus ignoring possible transfers to aquifers, the soil, and lakes. There is some evidence that transfers to lakes may be significant in enclosed basins in Tibet (Yao et al., 2007). By far the most important omission is the neglect of frontal ablation, which is shared by most other projections. Another feature that the mass-balance model shares with all glacier projections to have appeared so far is that it parameterizes ablation in terms of temperature rather than solving the glacier's energy and radiation balances explicitly. The complexity and attendant uncertainty of energy-balance modelling of glaciers on the global scale are, however, subjects for future research.

Some earlier projections were based on regional-scale analyses, but Radić and Hock (2011) are the first to describe regional variations in detail. They find that regional losses vary greatly. Expressed as percentages of initial mass, the final masses in 2100 range from $92\% \pm 4\%$ in Greenland and $90\% \pm 16\%$ in high-mountain Asia to $28\% \pm 7\%$ in New Zealand and only $25\% \pm 15\%$ in the European Alps. Complete disappearance of ice is projected in one region (the subantarctic islands), where the other nine models project 25%–80% losses. One model yields a projection of slight growth of glaciers in Iceland, one yields growth of 9% in Scandinavia, and four yield growth of up to 8% in high-mountain Asia (where the other six yield losses of up to 34%).

The largest contributions to the global Final SLR come from three regions with relatively moderate percentages of loss but large initial masses: arctic Canada (27 mm ± 12 mm SLE from an initial 199 mm ± 30 mm SLE), Alaska (26 mm ± 7 from 68 mm ± 8 mm) and Antarctica (21 mm ± 12 mm from 147 mm ± 64 mm). These losses are averages across the 10 GCMs used to drive the glacier models. Because the regional projections do not seem to exhibit strong central tendency, the ranges may be more informative about uncertainty in the climatic input projections: 6 mm–43 mm SLE for arctic Canada, 14 mm–36 mm for Alaska, 5 mm–41 mm for Antarctica.

8.6.1.9. Synthesis

The regularized projections agree in suggesting that mass loss over the twenty-first century is likely to contribute several tens to a few hundreds of millimetres of sea-level rise. The most recent and most detailed study (Radić and Hock, 2011) agrees well with the study that is likely to be cited most often in the near future (Meehl et al., 2007).

A notable observation about Figure 8.12 is that the more detailed studies tend to yield lower estimates of glacier mass loss while the higher estimates come from more generalized analyses. It would be a mistake, however, to conclude that the higher estimates are 'wilder' and that a fuller understanding of the problem brings more modest estimates. The modelling of physical processes in detail is possible only when initial and boundary conditions can be prescribed with some confidence. The climatic boundary conditions of this problem are supplied from GCMs, carrying all the uncertainty that is attached to climate projections, and the glaciological initial conditions, in particular the initial (2001) mass, are unsatisfactory in several respects. Moreover, detailed modelling presupposes detailed understanding, and some parts of the physical system are quite poorly understood. The interaction of glaciers with the ocean is the most obvious of these aspects.

An accelerating rate of loss per unit area from a store of diminishing areal extent entails a maximum in the total rate of loss. At first, the shrinkage does not counterbalance the increasing specific loss rate. Later, the continued increase of the loss rate fails to counterbalance the fact that there is less and less area remaining. The date of this maximum of total loss rate is of practical concern. Glacier meltwater is a growing resource for human activities before the maximum but a diminishing resource thereafter. Radić and Hock (2011) project a broad worldwide maximum of meltwater discharge over some decades centred on 2060 to 2080. In regional studies, Xie et al. (2006) assumed warming rates of 0.02 K and 0.03 K yr^{-1} for China and projected a broad maximum of discharge in 2020 to 2040, with rates remaining greater than in 2000 until 2050. Rees and Collins (2006) simulated mass balance in hypothetical glacierized drainage basins in the wetter eastern and drier western Himalaya. They imposed a warming rate of 0.06 K yr^{-1} and found that maxima of annual runoff would be reached around 2050 in the drier and around 2070 in the wetter climate.

It seems likely that glacier meltwater resources will become increasingly scarce beginning sometime in the middle of the twenty-first century, although it is also likely that the date of the inflection will vary by several decades from region to region. The meltwater resource is already scarce in regions such as the Cordillera Blanca of Peru and the basin of the Indus River, which no longer reaches the sea. Here, however, the scarcity is related not just to

climatic change but to the growing demand from a growing population, and possibly to imprudent management (cf. Taplin, 2012, this volume).

8.6.2. The Future of Himalayan Glaciers

A number of detailed single-glacier (e.g., Brown et al., 2010; J. Zhang et al., 2007) and regional (e.g., Zemp et al., 2006) projections of glacier evolution are available. The Himalayan region is of particular interest because of the importance of its glaciers as water resources for large populations and because of recent controversy.

Cruz et al. (2007) offered a case study of Himalayan glaciers to illustrate the impact of climatic change on Asia. Unfortunately, the study contained a number of errors. These errors were outlined by Cogley et al. (2010), but they were also the subject of intense scrutiny in the popular media during early 2010 (see Rice and Henderson-Sellers, 2012, this volume). Much of the journalistic and public attention focused on the derivation of the errors, which turned out to be traceable not to the peer-reviewed literature but to inaccurate reporting in an Indian popular science magazine of remarks by an Indian glaciologist that were later characterized as 'speculative'. For this aspect of the story, see Cogley (2011a).

The most significant of the Cruz et al. (2007) errors are in the statement in their section 10.6.2 (p. 493) that "Glaciers in the Himalaya are receding faster than in any other part of the world… and, if the present rate continues, the likelihood of them disappearing by the year 2035 or perhaps sooner is very high if the Earth keeps warming at the current rate." Setting aside some ambiguous repetition, and the fact that Himalayan glaciers are not receding more rapidly than glaciers elsewhere, the main problem here is that simple calculations suggest that the likelihood of disappearance by 2035 is extremely low, not "very high".

While it is easy to show that the speculative remarks that led to the Himalayan controversy cannot be right, it is considerably more difficult to produce reliable estimates of mass loss from Himalayan glaciers. A leading source of difficulty is lack of complete and reliable basic information. In early 2010, there was no complete inventory of the Himalayan glaciers and, where inventories of parts of the region were in existence and were accompanied by glacier outlines, the outlines were often poorly geo-referenced. The lack of accurate digital outlines makes it impossible to construct accurate area–altitude distributions from digital elevation models, and rules out more detailed glacio-climatic models that require hypsometric information as input.

The hypsometric barrier to progress has yet to be removed, but Cogley (2011a) reported on a reconnaissance inventory of the Indian part of Kashmir that fills the last remaining gap in the inventory of the entire mountain range. He went on to project the near future of Himalayan glaciers by relying on the two simple assumptions adopted earlier by Meier et al. (2007) for their global projections: constant rate and constant trend.

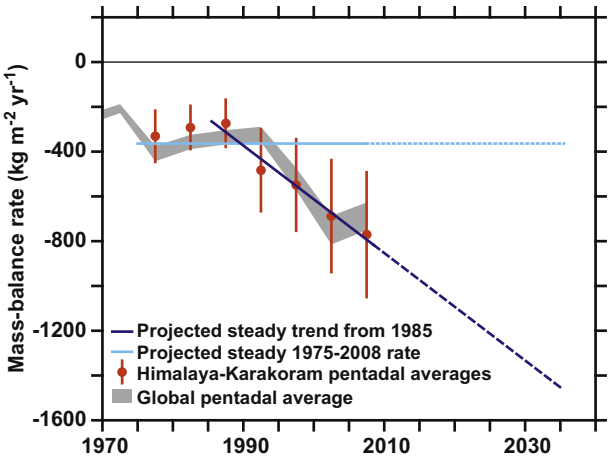

FIGURE 8.13 Constant-rate and constant-trend projections of the specific mass balance of glaciers in the Himalaya. The red circles are from a regional subset of $1° \times 1°$ cells extracted from the global pentadal averages (shown here in grey) of Figure 8.10b. *(Source: Cogley, 2011a, with permission. With kind permission from Springer Science + Business Media B.V.)*

The present mass-balance rate estimated by Cogley (2011b) (updating Cogley, 2009a) for the Himalaya–Karakoram region was -364 kg m^{-2} yr^{-1} over 1975/76–2007/08 (Figure 8.13), based on interpolation of a spatial polynomial from sparse local measurements and more distant measurements, the latter discounted by a distance–decay function. The trend (that is, the acceleration of the rate of mass loss) over 1985/86–2007/08 was -24.0 kg m^{-2} yr^{-2}; the beginning of the trend in the mid-1980s was chosen by eye. If the trend persists until 2035, the rate in that year will be about -1440 kg m^{-2} yr^{-1}.

The newly-complete glacier inventory made it possible to model glacier shrinkage as part of the projections, although at present it remains impracticable to incorporate the feedback of changing hypsometry on mass balance. Using the inverted thickness–area scaling equation (Equation (8.8)) and taking the mass-balance projections as measures of thickness change, it was possible to eliminate glaciers when their mean thicknesses diminished to zero. In turn, this made it possible to track the evolution of total glacierized area and total ice mass. The initial mass of each glacier is obtained readily from forward calculations of mean thickness, using Equation (8.5) and taking glacier area from the inventory. The dates of the inventory records vary from 1968 to 2003. The thickness–area scaling was used to synchronize them to 1985, and inventory records without dates were assigned to 1985.

Figure 8.14 shows the evolution of mass relative to mass in 1985, with projections for 2010 and 2035. A source of

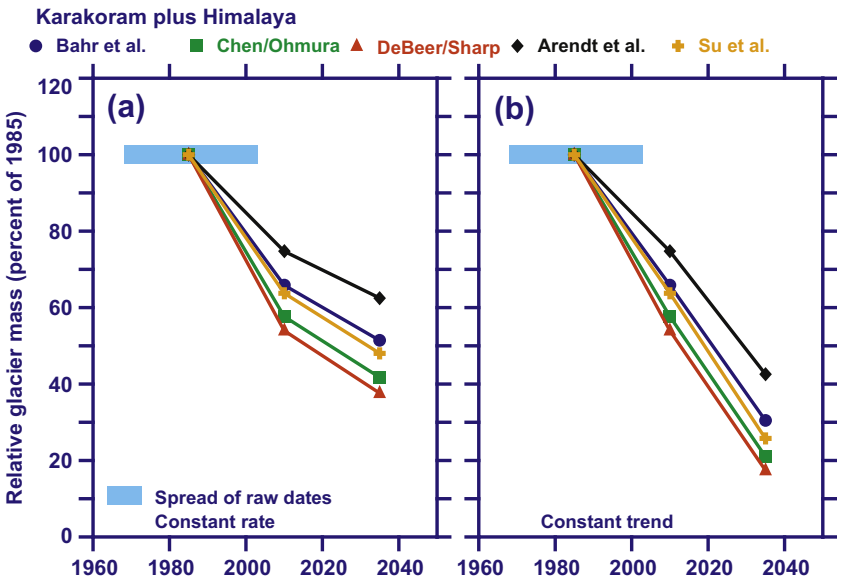

FIGURE 8.14 Constant-rate (a) and constant-trend (b) projections of the evolution of total glacier mass in the Himalaya, with allowance for the disappearance of individual glaciers as their mass balance is projected by thickness–area scaling (Section 8.4.1). The quantity plotted is the ratio of total mass to total mass in 1985, near the middle of the range of glacier inventory dates. Five plausible sets of thickness–area scaling parameters are used to illustrate the possible uncertainty of the projections: Bahr et al. (1997); Chen and Ohmura (1990); DeBeer and Sharp (2007); Arendt et al. (2006); Su et al. (1984). *(Source: Cogley, 2011b, with permission.)*

serious uncertainty is concealed by this method of presentation. None of the five sets of scaling parameters can be ruled out as implausible, but they yield total masses in 1985 that vary from 4000 Gt to 8000 Gt. That said, the pattern of evolution is the same for each parameter set. If mass loss proceeds at a constant rate (Figure 8.14a), the proportion of 1985 mass that may have been lost already is between a quarter and a half, while in 2035 the mass remaining will be between one and two thirds. The rate of loss is less from 2010 to 2035 because the glacier size distribution is evolving towards greater dominance by larger glaciers, as a consequence of the disappearance of smaller glaciers. If a constant acceleration of specific mass balance is assumed (Figure 8.14b), the faster specific rate of loss cancels out the impact of the changing size distribution, and the total loss rate remains nearly the same to 2035 as between 1985 and 2010. By 2035, between one fifth and two fifths of the 1985 mass remains.

This analysis is near to the crude end of the spectrum of sophistication, and urgently requires to be followed up with projections that describe more of the physical behaviour of glaciers and subject them to more realistic forcing. However, the analysis does have the merit of offering generalized early corrective guidance to resource managers and policymakers.

8.7. REFLECTIONS: GLACIERS AND THE FUTURE CLIMATE

8.7.1. Basic Information

A recurrent theme of the sections above has been the lack of basic information in readily usable form. For example, the work reported by Raper and Braithwaite (2005a) was necessary mainly because the World Glacier Inventory is incomplete. Many of the projections described above required similar time-consuming workarounds. Moreover, a problem not yet addressed in any projection is that the World Glacier Inventory is diachronous. Its component regional inventories span several decades, and rates of shrinkage are not well enough known for synchronizing information from different dates in an objective way. The initialization of glaciological projections is thus necessarily fuzzy.

Nevertheless, incremental advances in the completeness and usability of information proceed steadily. For example, digital elevation models of global or near-global extent and with spatial resolution adequate for glaciological modelling have become available in the past decade. They are ready and waiting to be masked by accurate glacier outlines, which are accumulating steadily also, although much labour remains. As the number of glaciers with mass-balance measurements increases unspectacularly, and the technology for mass-balance measurements improves more noticeably, surprising new results appear less often.

On the other hand, there are occasional surprises. Hock et al. (2009) modelled global average mass balance for 1960/61–2003/04 by estimating the sensitivity of mass balance to changes in temperature and precipitation. Glaciers in Antarctica stood out as leading contributors to a more negative global average than that of Lemke et al. (2007), due to their high sensitivity to temperature and the large warming in the vicinity of the Antarctic Peninsula. Local measurements being inadequate, the Antarctic estimates of Lemke et al. (2007) were based on an analogy with the high Arctic of Canada. This example illustrates the

growing importance of modelling, not just for investigating glacier futures but for understanding present and recent states of the glaciers. Although it compromises the mutual independence of glaciological and meteorological information about climatic change, modelling is becoming indispensable for the understanding of glacier mass balance. Further incremental advances in modelling methodology, for example for including glaciers in GCM simulations by subgrid-scale parameterization, should be expected and promoted.

8.7.2. Gaps in Understanding

Accuracy in projections of the future of glaciers is, of course, not limited solely by incomplete information. Glaciers share with the rest of the climate system all the dimensions of uncertainty about the future, and glaciology shares with climatology the attribute of incomplete understanding of the system under study.

Two examples of gaps in understanding of how glaciers evolve are the role of internal accumulation in polythermal glaciers (Sections 8.3.1 and 8.4.3) and the dependence of shrinkage rate on initial size (Section 8.5.3). In the first example, the gap is a roadblock because internal accumulation is extremely difficult to measure, at least economically. The result is that there are hardly any measurements, and no routine measurements, and consequently that the only practical approach is to model the phenomenon. However, the models have almost no observational support for calibration, and the problem is thus circular — and persistent. In the second example, the gap takes the form of not knowing why the shrinkage rate depends exponentially on the initial area (that is, why smaller glaciers shrink faster). An exponential dependence on area suggests that the answer might lie in linear behaviour of one horizontal dimension, presumably the glacier length. This phenomenon is made more puzzling by the failure of some glacierized regions to exhibit it and, in more typical regions, by the extreme variability of the shrinkage rates of the smallest glaciers in any representative sample. Their short response times may play a role; but a safe generalization is that the gap in understanding is there because the problem has been little studied hitherto.

The largest single impediment to intellectual progress on the behaviour of glaciers, however, is tidewater instability (Meier and Post, 1987). This term describes unsteady behaviour of a calving glacier that alternates between episodes of slow advance and rapid retreat. Outside the ice sheets, timescales appear to be centuries for advance and decades for retreat. Timescales are not known for the ice streams that discharge much of the ice from the ice sheets, except that some very large ice streams are suffering very rapid retreat at the present day. The conditions permitting advance in the first place, and the triggers for subsequent unstable retreat, are both poorly understood. Once retreat has begun, however, observation and numerical simulation (Schoof, 2007) agree that, if the bed is grounded below sea level but has a slope opposed to that of the surface, the retreat will continue until the calving front or grounding line reaches a part of the bed that slopes in the same direction as the surface. During this unstable retreat, enhanced calving leads to a positive feedback in which accelerated flow and dynamic thinning extend far upglacier from the part that is grounded below sea level. Mass loss is far greater than, and essentially independent of, the climatic mass balance.

It is difficult, however, to refrain from suspecting a role for climatic change, direct or indirect, in the dramatic changes being exhibited at present by many tidewater glaciers. Steffen et al. (2008, p. 30) assessed the interaction of warm seawater with the peripheries of the ice sheets as "a strong potential cause of abrupt change", an assessment reinforced, for example, by the observations of Rignot et al. (2010). Tidewater instability was described long ago by Weertman (1976, p. 284) as "glaciology's grand unsolved problem". It remains unsolved today, but it is the subject of intense current effort because we cannot assess the probability that large parts of one or both of the ice sheets might collapse into the sea.

8.7.3. The Probability Distribution Function of Glacier Futures: Glimpses of the Known and Unknown

Wigley and Raper (2001) argue that a climatic projection presented as a range may be misleading unless it is accompanied by some guidance as to what the range means in terms of probability. They suggest a four-step procedure for providing such guidance: 1) identify the main sources of uncertainty; 2) represent each of these input uncertainties as a probability distribution function; 3) draw samples from the probability distribution function to drive the model that is to generate the projection; 4) construct an output probability distribution function from the results of step 3. In glaciology at present, this quasi-Bayesian approach breaks down at step 2, because we are unable even to sketch distribution functions for some of the least well-known uncertainties. Step 3 is also problematic in that some of the processes that are at work are understood well enough that models for them are stable and reliable but, for others, especially frontal ablation, it is not yet possible to write down the governing equations in a practicable way.

Nevertheless, the synthesis attempted above does hint at what an output or posterior probability distribution function for mass loss from glaciers might look like. None of the projections are less than 60 mm SLE for the twenty-first century, and the lowest projections appear to have low or

very low probability because they underestimate initial glacier mass. The most recent and most detailed projection (Radić and Hock, 2011) is that the twenty-first century contribution to sea-level rise from glaciers other than the ice sheets is more likely than not (in IPCC terminology) to lie between about 90 mm and about 160 mm SLE. It is in general agreement with two earlier IPCC assessments that were more generalized, but were diverse in approach. The highest recent estimates are from calculations that are even more generalized, although they can be seen as tentative descriptions of the upper tail of the probability distribution function.

When the total length of calving glacier margins becomes known more accurately, it is likely that the higher estimate of Pfeffer et al. (2008) will be ruled out. It will probably be found that, even if the present-day calving margins could be maintained in spite of retreat, there is not enough ice tributary to such margins to supply the projected cumulative ice discharge. However, the lower end of the Pfeffer et al. (2008) range will not be so easy to dismiss in this way, and indeed its estimate of frontal ablation addresses a known and significant unquantified omission from all of the detailed projections. For a different reason, the projections of Bahr et al. (2009) are also not dismissible. They address the undoubted fact that some of the response of glaciers to climatic change is 'buried' in their geometric behaviour (delayed shrinkage towards equilibrium sizes), a fact that is addressed only indirectly or, in some cases, not at all in other projections. The higher Bahr et al. (2009) projection was obtained quite crudely and on that ground should be assessed as less probable than the lower projection, but the lower projection suffers from the basic flaw that it assumes a highly improbable unchanging climate.

Table 8.1 and Figure 8.12 present ranges, rather than central values with confidence envelopes. The latter style would mislead by suggesting a known probability distribution function, especially if the confidence region were represented with the '±' symbol. For the future of glaciers, the output probability distribution function envisaged by Wigley and Raper (2001) is not known, except that it seems to be asymmetrical. Small losses are less probable than large losses over the twenty-first century. Asymmetrical probability distributions in the climate system were discussed by Urban and Keller (2009), who suggested that they might arise from incomplete understanding, rather than from the system itself. Whether the apparent glaciological asymmetry will turn out to be intrinsic or just an artefact of the incomplete glaciological understanding described here is an open question.

ACKNOWLEDGEMENTS

I thank Regine Hock and an anonymous reviewer for detailed and constructive comments.